Southeastern Geology: Volume 39, No. 1 November 1999

Editor in Chief: S. Duncan Heron, Jr.

Abstract

Academic journal published quarterly by the Department of Geology, Duke University.

SOUTHEASTERN GEOLOGY

PUBLISHED

at

DUKE UNIVERSITY

Editor in Chief:

Duncan Heron

This journal publishes the results of original research on all phases of geology, geophysics, geochemistry and environmental geology as related to the Southeast. Send manuscripts to **DUNCAN HERON, DUKE UNIVERSITY, BOX 90233, DURHAM, NORTH CAROLINA 27708-0233**. Phone: 919-684-5321, Fax: 919-684-5833, Email: heron@eos.duke.edu Please observe the following:

1) Type the manuscript with double space lines and submit in duplicate.
2) Cite references and prepare bibliographic lists in accordance with the method found within the pages of this journal.
3) Submit line drawings and complex tables reduced to final publication size (no bigger than 8 x 5 3/8 inches).
4) Make certain that all photographs are sharp, clear, and of good contrast.
5) Stratigraphic terminology should abide by the North American Stratigraphic Code (American Association Petroleum Geologists Bulletin, v. 67, p. 841-875).

Subscriptions to *Southeastern Geology* for volume 39 are: individuals - $19.00 (paid by personal check); corporations and libraries - $25.00; foreign $29. Inquires should be sent to: **SOUTHEASTERN GEOLOGY, DUKE UNIVERSITY, BOX 90233, DURHAM, NORTH CAROLINA 27708-0233**. Make checks payable to: *Southeastern Geology.*

Information about SOUTHEASTERN GEOLOGY is on the World Wide Web including a searchable author-title index 1958-1996. The URL for the Web site is:

http://www.geo.duke.edu/seglgy.htm

SOUTHEASTERN GEOLOGY is a peer review journal.

ISSN 0038-3678

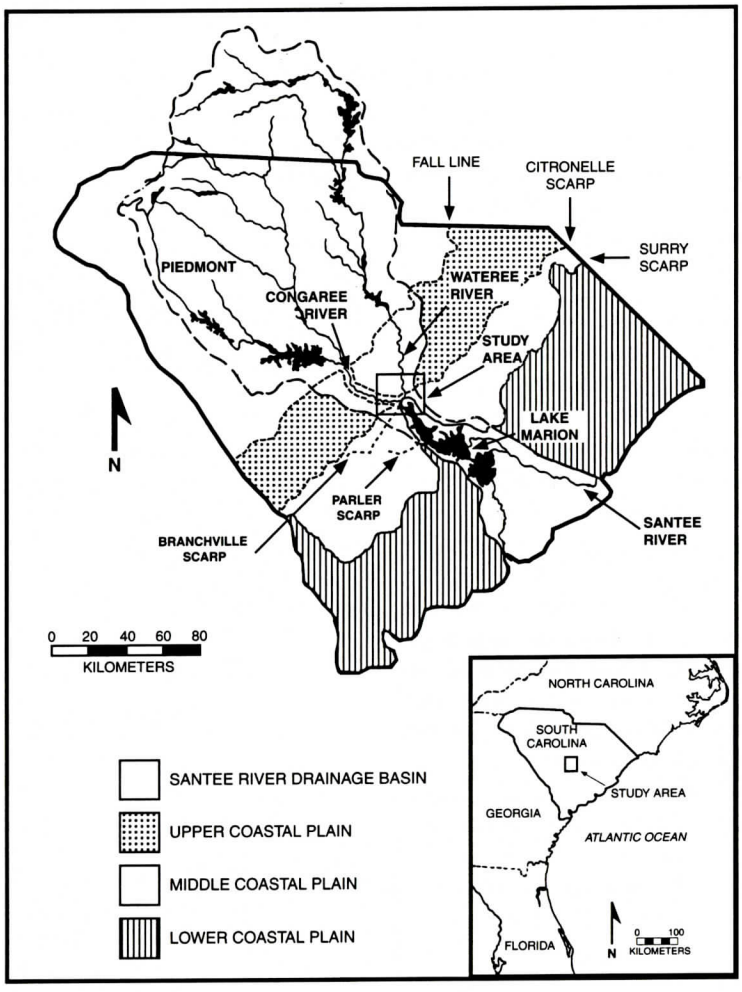

Figure 1. Regional location map for the study area. The study area is located in South Carolina at the contact between the Upper and Middle Coastal Plains where the Congaree and Wateree Rivers meet, forming the Santee River. The Santee River drainage basin includes most of the Piedmont of South Carolina and a portion of the Appalachian Mountains.

of Leopold and Maddock (1953), are nearly at grade, having experienced a near constant base level (i.e., mean sea level) for essentially the past 4,000 to 5,000 years. The alluvium in the aggraded valley is the ideal bed material for a river to adjust slope in a flood plain which signals the achievement of grade (Bloom, 1978). These systems have, and can maintain, grade by adjusting factors such as channel width and channel depth with their available grain size (Leopold and Maddock, 1953).

The goal of this study was to investigate the valleys' geomorphological character as it applies to river channel stability, with emphasis placed on the Santee River. Little detailed geological information is available for the valleys within the study area, therefore baselevel data was collected. Points of interest were; will the river channels in the future migrate as a channel form across the alluvial valley, or will the channels tend to relocate due to channel abandonment? To study these alluvial valleys, detailed topographic mapping, riverine morphology studies, sediment analysis, and historical mean-

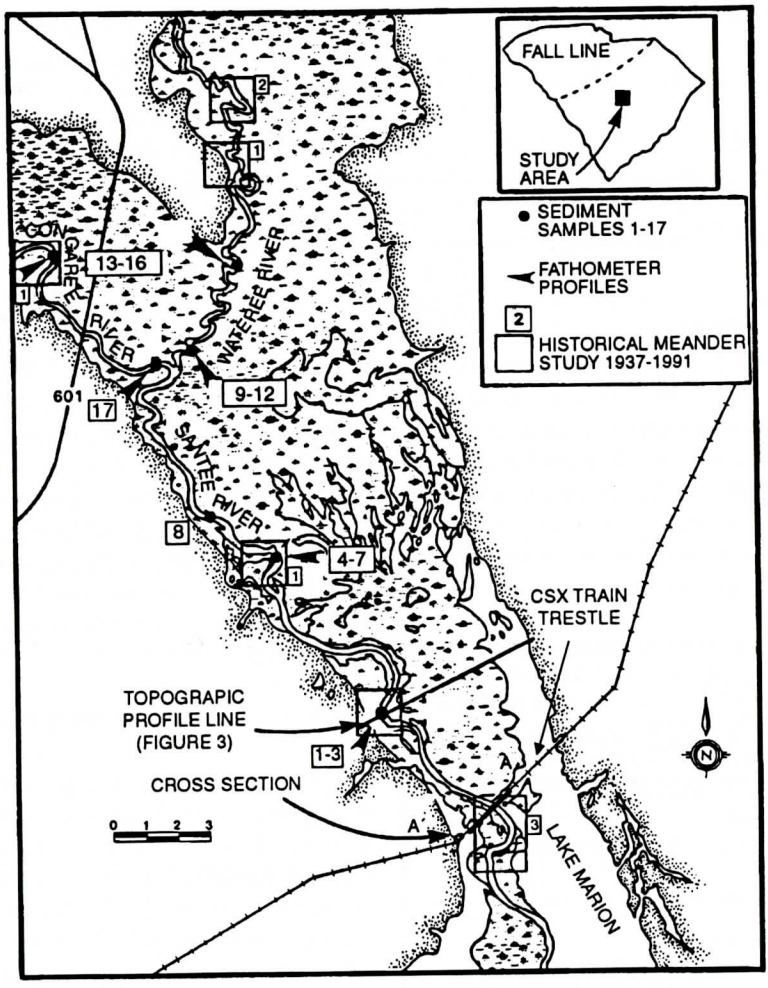

Figure 2. Detailed location map of the study area which includes the Santee, Congaree, and Wateree River alluvial valleys. Located on this map are the meander bends studied (historical meander rates, sediment samples collected), topographic survey line, and geologic cross-section.

plain. Through time, this overbank levee deposition will cause the Santee River to become topographically higher than the remainder of the flood plain. This sets the stage for possible abandonment and relocation of the river channel within the valley.

A total of 79 sediment and shallow auger (<1m) samples were collected along the topographic profile line across the Santee River Valley. At these 79 sample sites, 26 shallow hand auger borings were made to describe the shallow subsurface sediments. Sand size material was encountered at only four of the sample sites across the entire 4.2 km wide flood plain, excluding the active Santee River. The remainder of the sediment samples across the floodplain were principally silt and clay. Sandy sediments (fine-medium grained) mixed with silt and clay were sampled adjacent to either side of the active Santee River and in the small channels of two creeks that bisect the flood plain. The typical sediment sampled in the flood plain was a rooted silt and clay that changed in color from grey to mottled tan/orange with depth. Also, in varying degrees, organics and evidence of bioturbation were observed, typically near the surface, and the fine grained sediments became drier and more compact with depth.

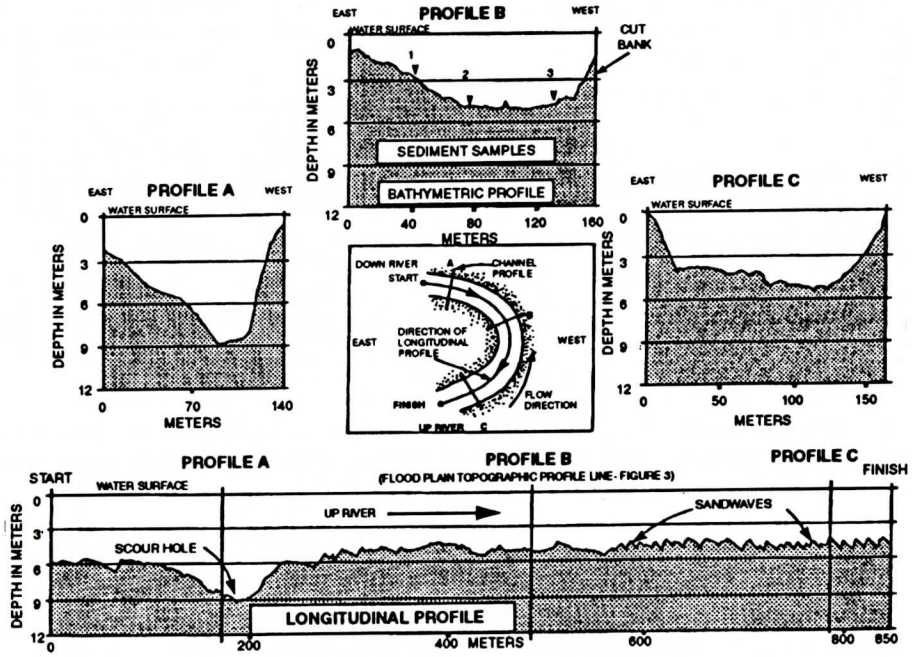

Figure 4. Fathometer profiles for meander bend #2 on the Santee River at the point where the topographic profile crosses the river. A total of four profiles were run for each of the six meander bends studied. Sediment samples were collected along profile B, and note the numerous bedforms migrating down river on the longitudinal profile.

bar side of the river (east) gently sloping down into the thalweg and abruptly rising onto the cut bank. The riffle channel cross-sections between meander bends of the Santee River most often exhibited a more U-shaped channel profile than the meander bends. Generally, the Santee River channel has a depth of 5 to 7 meters.

A total of 17 sediment samples were collected and analyzed (Folk, 1974) from the three river systems (Table 3). Generally, samples were collected across the channel at the apex (profile B, Figure 4) for a given meander bend. The sediments in the Santee River, located along the topographic profile line labeled #2 (Figure 2), had a grain size pattern often observed in the field at other point bars on the Santee River. At the meander bend #2 on the Santee River, a well-sorted fine sand mixed with a moderate amount (20%) of silt and clay were sampled at the beach located along the bank attached to the point bar. On the point bar side of the channel, the sediments in the channel were a medium-to-coarse sand that was moderately well-sorted. In the straight channeled (riffle) areas of the river, a variety of sediments were sampled ranging from medium sand to pebble-sized gravel. On the cut bank side of the river at meander #1 on the Santee River, pebble-sized gravel was sampled (Table 3).In general, if the sediments sampled in the river were stacked vertically due to lateral migration of the channel, a fining-up sediment sequence would be produced, although the middle of the deposit would be uniform.

To further define the morphological characteristics of the river systems, the sinuosity index and channel width-to-depth ratios were calculated for each river (Table 4). The sinuosity index for each river was measured from the confluence of the Congaree and Wateree Rivers (Figure 2). For each river, 20 km of linear flood plain was measured and then compared to the length of meandering river within that reach, to determine the sinuosity index. The Santee River has a sinuosity index of 1.37 as measured, which indicates that the river tends more toward

Table 4. River channel morphological measurements from each alluvial valley. Sinuosity index was measured from the point where the Congaree and Wateree meet. The second Wateree sinuosity index was measured for the final 6 km of the river prior to joining the Congaree River.

River	Flood Plain Distance Measured (km)	Sinuosity Index	Channel Width to Depth Ratio
Santee	20	1.37	28.5
Congaree	20	1.75	47.5
A.Wateree	20	1.73	20.7
B. Wateree	6	1.82	Not Measured

CONGAREE RIVER

The Congaree River is larger than the Wateree River (Table 1) and the two rivers join within the study area to form the Santee River (Figure 2). The flood plain of the Congaree River was not surveyed in detail as part of this study, although the author has made numerous field observations of the Congaree River Flood Plain while leading geological field seminars, and conducting both environmental and geological research projects. Generally, the surface sediments of the flood plain of the Congaree River are similar to the Santee River, except the Congaree River flood plain is not permanently flooded. The upper reach of the Santee River has been flooded since the construction and flooding of Lake Marion during the early 1940's. The surface of the flood plain is predominantly silt and clay with sand occurring only in small creeks that cross the flood plain and in the immediate vicinity of the active Congaree River. The historical study on the Congaree River indicated that these meander bends have migrated more rapidly than those on the Santee River. The average meander rates per year for the meanders studied on the Congaree River (1.8 m/yr) were nearly twice that of the Santee River (1.0 m/yr, Figure 2). Only one meander bend on the Congaree was surveyed in detail in the field during this study. At this meander bend and in other straight sections of the river, water depths in the Congaree River were generally shallower than the Santee River, ranging from 3 to 5 meters. The Congaree River was also slightly wider than the Santee River. Overall channel morphology was similar to that found on the Santee River as discussed previously and shown on Figure 4.

Sediments sampled from the Congaree River were finer-grained than the sediments sampled from the Santee River (Table 3). Sediments from the Congaree River were also more uniform, lacking the range of grain size than that sampled on the Santee River. A previous study on deposits of the upper reach of the Congaree River (Levey, 1978) found coarse-to-medium sand as the most common sediment size on the point bars. Some point bars studied by Levey had moderate amounts of gravel present, more often found on the upstream (proximal) end of the bars.

The sinuosity index was measured for the Congaree River using the same methodology described for the Santee River. The sinuosity index calculated for the Congaree River was 1.75 (Table 4). This is precisely the same sinuosity index Levey (1977) calculated for the upper portion of the Congaree River near the Fall Line. With a sinuosity index of 1.75, the Congaree River is a good example of a meandering river.

The width/depth ratio of the Congaree River was 47.5 (Table 4), which indicates the Congaree River is tending more toward a bed load river. This value for the width/depth ratio was calculated using a small data base, and further investigation is warranted.

WATEREE RIVER

The Wateree River has a smaller drainage basin and its discharge is less than either the Congaree or Santee Rivers (Table 1). Field studies of the Wateree River flood plain were not undertaken as part of this study. Only the river channel was investigated. The author has limited field experience in the flood plain of the Wateree River. Based on that limited experience and the review of aerial photography, it is felt that the flood plain is somewhat similar to those

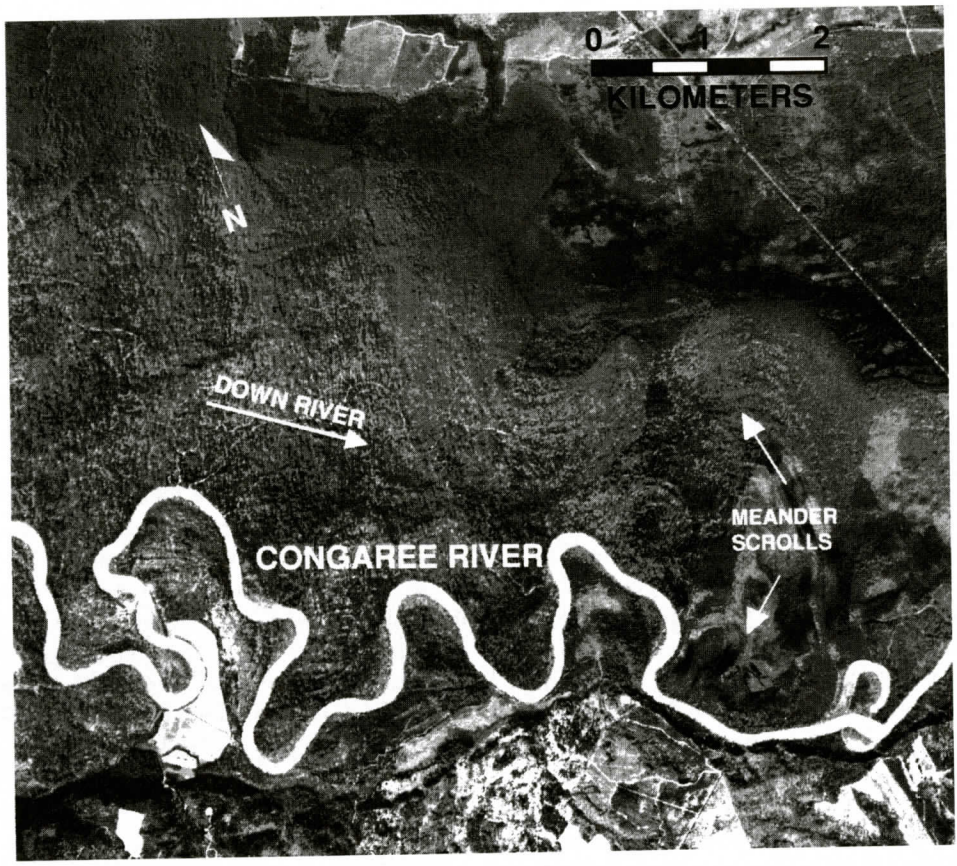

Figure 5. Vertical aerial photograph of Congaree River just prior to joining the Wateree River. This valley is asymmetric to the southern side of the valley and is a good example of a meandering river (scale, 1 cm = 400 m, photo taken March 1991).

elevations reaching 200 feet above mean sea level, in contrast to the northeast valley wall which has an elevation of only 90 feet above mean sea level. The lower portion of the Congaree River that was studied was very similar to the upper portion of the river previously studied by Levey (1978). Essentially, the entire valley of the Congaree River has evidence of past river channel migration denoted by abundant meander scrolls across the entire flood plain (Figure 5).

Located within the upper portion of the Santee River alluvial valley there is a pattern of former multiple channels located in the center of the flood plain (Figure 7). These channels begin two miles down the flood plain after the confluence of the Congaree and Wateree Rivers. This drainage pattern appears to be braided and extends downstream toward the narrowest portion of the Santee River valley (Figures 2 & 7). The braided channel area encompasses approximately 3 square kilometers in the flood plain. One possible explanation for the braided channel pattern may be that the flood plain in this area is experiencing a slope change which could alter the channel form within the valley. Another possible explanation for the multiple channel braided pattern is inherited topography formed during the Wisconsin. This channel pattern is similar in appearance to present day alluvial fans or a braided stream morphology. It would only take a small elevation difference to produce the slope necessary to develop this type of drainage pattern in such a low-relief environ-

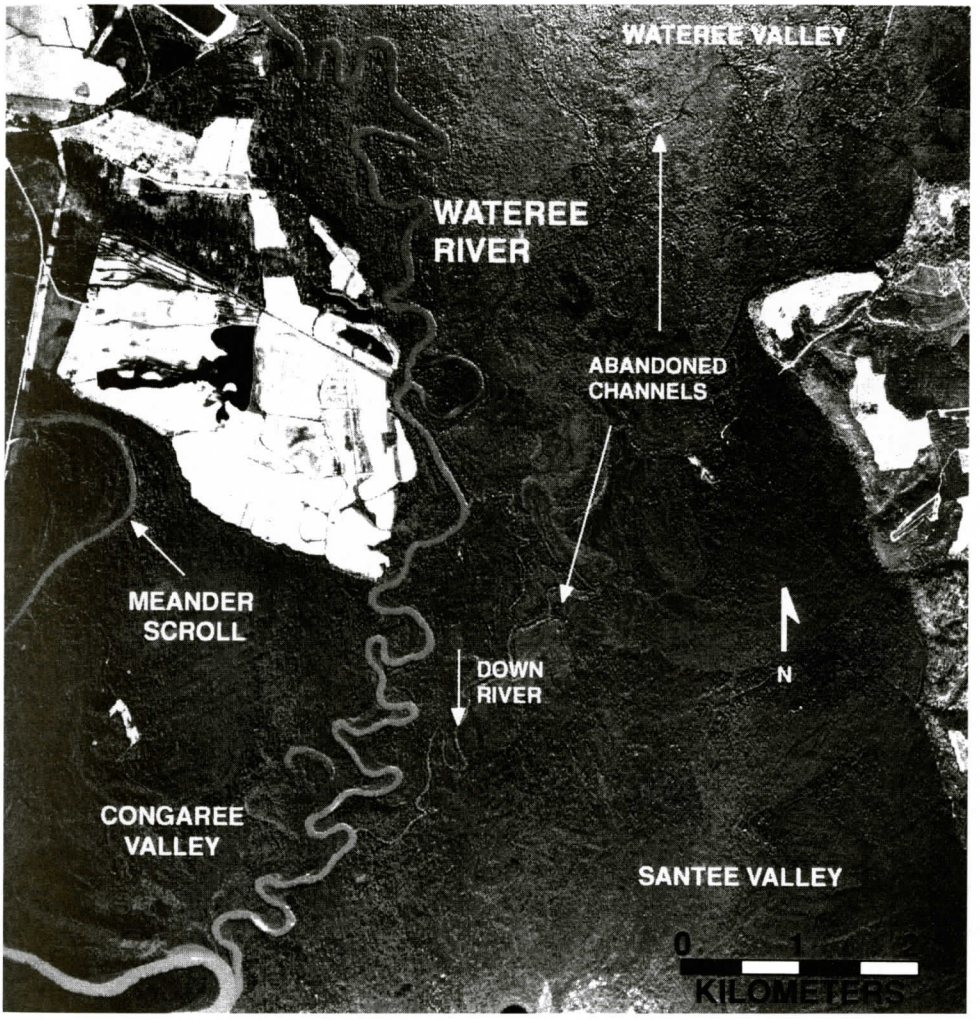

Figure 6. Vertical aerial photograph of the Wateree River valley as it joins the Congaree River. The Wateree River has numerous tight meander bends which increase in occurrence just prior to joining the Congaree River (scale, 1 cm = 400 m, photo taken February 1991). This alluvial valley is characterized by numerous abandoned (underfit) channels.

ment as a flood plain.

Several meander scrolls that extend for approximately 1 to 2 kilometers are present in the Santee River flood plain, once beyond the braided channel area discussed above. It does not appear that the flooding of Lake Marion has significantly altered the very uppermost reaches of the Santee River. The meander bends on the Santee River are still active, and the overall straight nature of the Santee River channel (both before and after the flooding of Lake Marion), indicates that the river system is behaving very similar to that before the flooding of the lake.

As part of this investigation, foundation borings for the CSX train trestle were obtained for a portion of Santee River alluvial valley in the vicinity of the active Santee River (Figure 2). The data consisted of borings drilled in 1968 and 1969. The geological descriptions made during these investigations are shown in the stratigraphic cross-section A-A' (Figure 8). The lithologic units have been generalized due to the quality of the data. The location of cross-

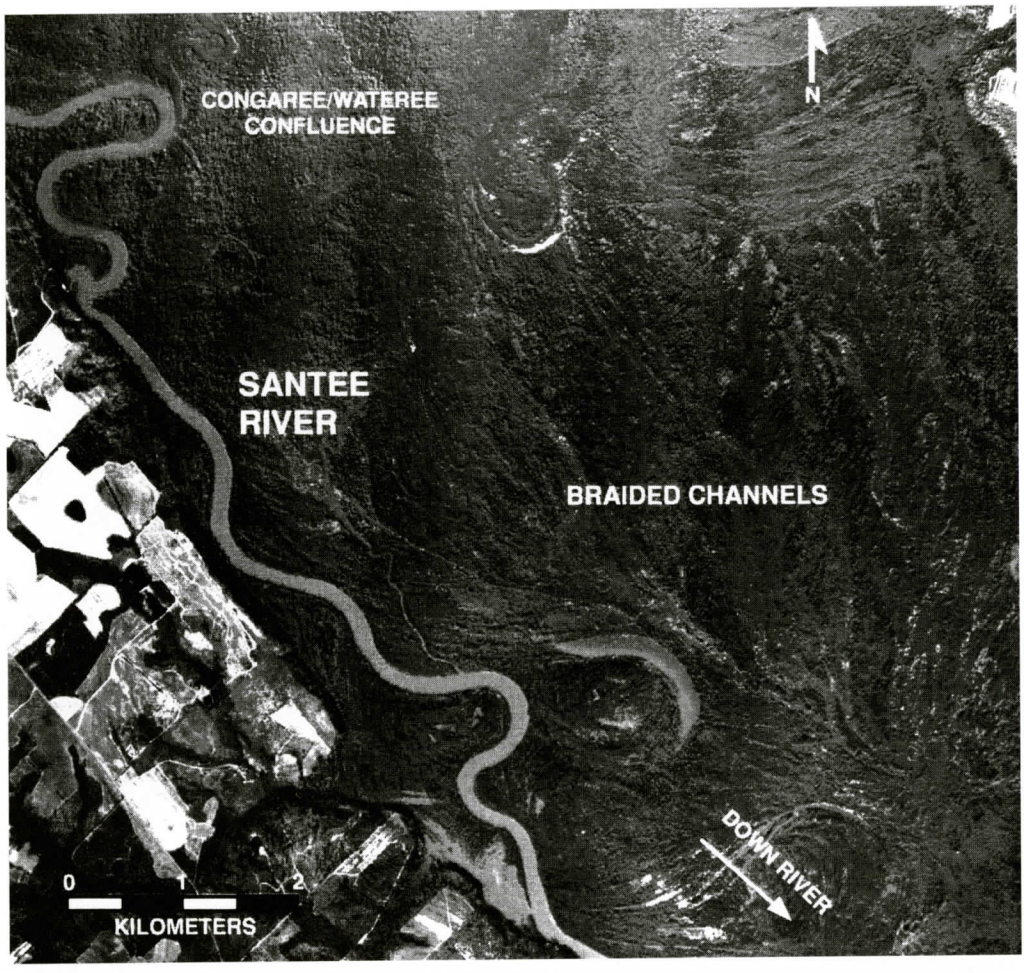

Figure 7. Vertical aerial photograph of the Santee alluvial valley just after the Congaree and Wateree Rivers meet. The Santee River tends toward a straight channeled river system within the study area (scale, 1 cm = 400 m, photo taken February 1991). Note the braided channel network at the center of the alluvial valley.

section A-A' is generally in the center and to the western side of the Santee River Alluvial valley (Figure 2). There is a silt and clay/hardpan which is typically at 10 m below the present flood plain surface except at the deep scour on the cross-section where it occurs at 15 m below the flood plain. Above this hardpan, 5 m thick fine-to-coarse sand is nearly continuous across the valley. Coarse sand and gravel were sampled in the deeper scours located more in the center of the alluvial valley and on the western end of the cross-section. These sand deposits appear to be uniform to slightly fining up sequences. Directly above the deep scour on the cross-section is recent abandoned Santee River channel fill. This deposit is composed of a sand dominant, point bar/channel and mud-filled oxbow. The present day Santee River lies to the west, which is southwest of both of these previous channel positions. This may indicate recent westerly migration of the river system in the valley.

The three alluvial valleys are similar in that they have active river channels located on the far western/southern sides of the valleys with a mud dominant flood plain. The present position

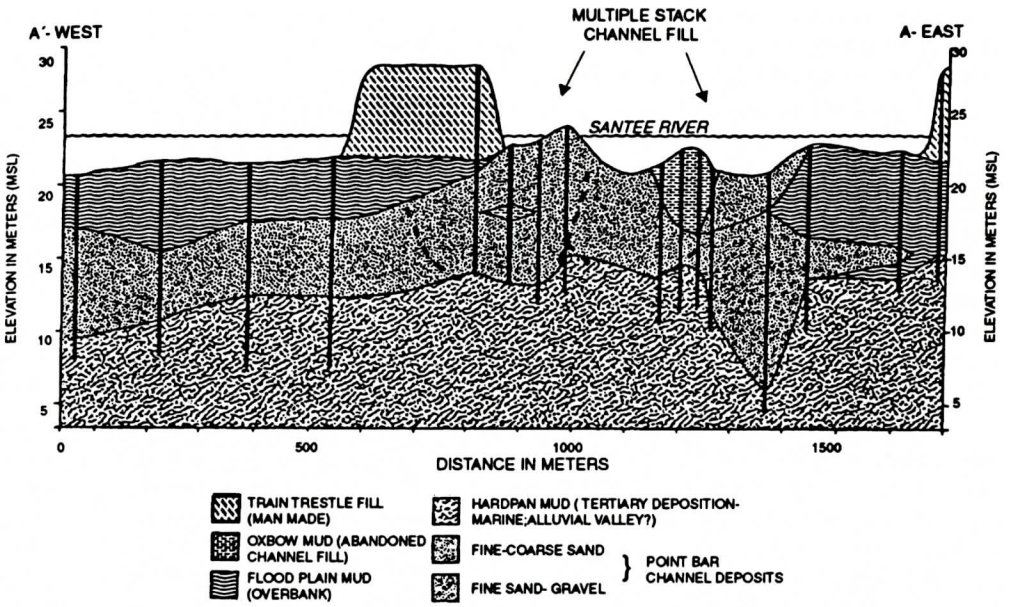

Figure 8. Geological cross-section of a portion of the Santee River alluvial valley. This cross-section is based on a series of borings made from the CSX train trestle and located on (Figure 1). The alluvial valley has abundant sand above a silt and clay (hardpan) deposit. The valley also has several channel fill sequences preserved in the near vicinity of the active Santee River.

of the rivers and limited subsurface data indicates lateral movement of the rivers in a southwesterly direction. This is similar to the movement of the Savannah River as described by Leeth and Nagle (1996). In their paper, Leeth and Nagle hypothesized that tectonism is possibly responsible for the lateral migration of the Savannah River. Other similar research (Prowell and Obermcien, 1991 and Soller, 1988) stated that the southwestern migration of the Cape Fear River, North Carolina, is due to uplift at the northwest-southwest trending Cape Fear Arch. Based on data gathered during this study and previous field experience in the study area, it is felt that the valleys are impacted by a tectonic element. The Cape Fear Arch is the most likely known tectonic element in the region that would have such an impact on our study area.

The Alluvial valleys are similar in that they are all well defined with extensive Flood plain deposits, although their rivers contrast significantly. The Santee River is essentially a straight channeled river whereas the Congaree and Wateree Rivers are good examples of meandering river systems. Of the three rivers, the Wateree is most unique with the numerous underfit channels in the flood plain, uniform sediment distribution in the river, and its highly meandering nature.

This particular section of the coastal plain of South Carolina is very dynamic in that three large river systems are changing gradient, leaving the upper coastal plain flowing down onto the middle coastal plain within a small geographic area. This resulting break in coastal plain slope produces a diverse morphological setting in these alluvial valleys

CONCLUSIONS

This study documents sediment trends and alluvial valley geomorphology at the point where the Congaree and Wateree Rivers join to form the Santee River. These rivers are mixed load rivers, and the Congaree and Wateree Rivers have meandering channels while the Santee River channel is a relatively straight river. The topographic profile across the Santee River Al-

luvial valley revealed that overbank levee deposition is elevating the Santee River above the flood plain, setting the stage for future channel relocation and abandonment. Sediments in the rivers vary from fine sand to pebble-sized gravel while the flood plains are silt and clay dominant. Bedforms were more frequent in the larger Congaree and Santee Rivers. Of the three rivers, the Wateree River is the smallest and differs most with a limited range in grain size, numerous abandoned channels, and frequent meander bends. All of the active river channels are presently on the southwestern side of the alluvial valleys. This may be a product of a tectonic gradient generated by the Cape Fear Arch that is responsible for this lateral migration. The Santee River alluvial valley has a pronounced unconformity at 10 to 15 meters below the present floodplain surface.The sediment above this unconformity most likely represents late Pleistocene and Holocene valley aggradation. Each river system exhibits its own geomorphological signature/pattern ranging from large meander scrolls (Congaree) to underfit channels (Wateree) to braided channel patterns (Santee), making for a complex geomorphological setting.

ACKNOWLEDGMENTS

I would like to thank Mark Whittle and Gary Padgett with the ETE Division of the Viro Group Inc. for field assistance and logistical support. I would also like to thank Miles Hayes, Tom Moslow and Peter Haff for their insightful reviews of this manuscript. I would also like to thank Neil Wicker for production of figures, Amy Hausser and Caroline Jenkinson for editing and production support, Mike Bise for field assistance and drafting, and Glenn Christenson for data analysis and field assistance. Funding for this project was provided by Laidlaw Environmental Services and Athena Technologies, Inc.

REFERENCES CITED

Bennett, C.S.and others,1993, U.S. Geological Survey Water-Data Report SC-92-1: United States Geological Survey, Water Resources Div., Columbia, SC, 480 pp.

Bloom, A.L., 1978, Geomorphology: Englewood Cliffs, NJ, Prentice-Hall, 510 p.

Colquhoun, D.J., 1974, Cyclic surficial stratigraphic units of the Middle and Lower Coastal Plains, Central South Carolina, *in* Oaks, R.Q, and Dubar, J.R., eds., Post-Miocene Stratigraphy Central and Southern Atlantic Coastal Plain: Logar, Utah, Utah State P, 1974, p. 179-190.

Dole, R.B., and H. Stabler, 1909, Denudation: USGS Water Supply Paper 243, p. 78-93.

Folk, R.L., 1974, Petrology of sedimentary rocks: Austin, TX, Hemphill Publishing Co., 182 p.

Jackson, II, R.G., 1975, Velocity-bedform-texture patterns of meander bends in the lower Wabash River of Illinois and Indiana: Geological Society of America Bulletin, v. 86, p.1511-1522.

Leeth, David C., and Nagle, Douglas D., 1996, Shallow subsurface geology of part of the Savannah River alluvial valley in the Upper Coastal Plain of Georgia and South Carolina: Southeastern Geology, Vol. 36, p. 1-14.

Leopold, L.B., Wolman, M.G., and Miller, J.P., 1964, Fluvial Processes in Geomorphology: San Francisco, W.H. Freeman and Co., 522 p.

Leopold, L.B., and Maddock, T., 1953, Hydraulic geometry of stream channels and some physiographic implication: United States Geological Survey, Professional Paper 252, 57 p.

Leopold, L.B., and Wolman, M.G., 1957, River channel patterns; braided, meandering and straight: United States Geological Survey Professional Paper 282-B, p. 39-85.

Levey, R.A., 1977, Characteristics of coarse-grained point bars, Upper Congaree River, South Carolina: unpublished M.S. thesis, University of South Carolina, Columbia, 61 p.

Levey, R.A., 1978, Bedform distribution and internal stratification of coarse-grained point bars, Upper Congaree River, S.C., *in* Miall, A.D., ed., Fluvial Sedimentology: Canadian Society of Petroleum Geologists, Vol. 5, p. 105-128.

Prowell, D.C., and Obermeier, S.F., 1991, Evidence of Cenozoic tectonism, *in* Horton, J.W., Jr., and Zullo, V.A., eds., Geology of the Carolinas: Carolina Geological Society 50th Anniversary volume, p. 309-318.

Rust, B.R., 1978, A classification of alluvial channel systems, *in* Miall, A.D., ed., Fluvial Sedimentology: Canadian Society of Petroleum Geologists, Vol. 5, p. 187-198.

Schumm,S.A., 1977, The fluvial system, 338 p.New York: Wisley & Sons.

Schumm, S.A., 1972, Fluvial paleochannels, *in* Rigby, J.K., and Hamblin, W.K., eds., Recognition of Ancient Sedimentary Environments: Society of Economic Paleontologists and Mineralogists Spec. Pub. No. 16, p. 98-107.

Schumm, S.A., 1968, Speculations concerning paleohydrologic controls of terrestrial sedimentation: Geologic Society of America Bulletin, Vol. 79, p. 1573-1588.

Soller, D.R., 1988, Geology and tectonic history of the lower

Cape Fear River valley, southeastern North Carolina:United States Geologic Society Professional Paper 1466-A, 60 p.

South Carolina Research Planning and Development Board,1948, Summary of Records of Surface Water Supply of South Carolina 1884-1946,Columbia SC, United States Geologic Survey Department of the Interior,188 p.

SOUTHEASTERN GEOLOGY
V. 39, No. 1, November 1999, p. 17-35

COMPOSITIONAL VARIATION IN THE GRANOPHYRE-RICH FARMVILLE DIKE, A MESOZOIC DIABASE IN SOUTH-CENTRAL VIRGINIA

FRANCIS Ö. DUDÁS[1] AND PHILIP T. ROGAN[2]

Department of Ocean, Earth and Atmospheric Sciences
Old Dominion University
Norfolk, VA 23529

[1] Now at: Tark Geosciences, 9 Lakeside Road, Billerica, MA 01821

[2] Now at: Jones Technologies Inc., 813 Forrest Dr., Suite C, Newport News, VA 23606

ABSTRACT

A 150-m wide Mesozoic diabase dike near Farmville, VA, is strongly zoned from granophyre-bearing margins to a 30-m wide granophyre-rich core. The main mass of the dike averages 15 vol.% granophyre, whereas the core contains 35 vol.%. The transition from granophyre-poor to granophyre-rich diabase occurs over < 6 m. Granophyre is dispersed throughout the dike and does not form continuous zones. Hydrothermal alteration is pronounced near granophyre patches. Modal zoning is reflected in compositional zoning: in the main dike and the core, respectively, SiO_2 averages 52 and 58 wt.%. Phase equilibrium modeling shows that, excepting SiO_2, TiO_2, K_2O and Ba, elemental variations are consistent with closed system fractional crystallization. Isotopic compositions require two different isotopic components and clearly indicate open system behavior in the dike. The contaminant component had higher Rb/Sr and lower Sm/Nd and U/Pb than the parental diabase. These isotopic patterns suggest anatexis of rocks isotopically similar to those of the Milton Belt of North Carolina, probably at mid-crustal levels. Fractional crystallization, assimilation, magma mixing and hydrothermal alteration contributed to compositional variation in the Farmville dike. The compositional contrast between the granophyric core and the main mass of the dike reflects either continuous tapping of a compositionally stratified magma chamber, or multiple intrusion.

INTRODUCTION

Mesozoic basalts and diabases along the eastern margin of North America record events associated with opening of the Atlantic Ocean (Puffer, 1992). Though this igneous province is volumetrically small in contrast to other rift-related suites (e.g., the Parana), literature on the Mesozoic diabases is extensive (Froehlich and Robinson, 1988; Puffer and Ragland, 1992), focusing primarily on the mechanisms that produced compositional variation in the rocks. Recent studies recognize that crustal contamination affected some of them (e.g., Philpotts and Asher, 1993; Puffer and Benimoff, 1997), but assessment of the interaction of crust with mantle-derived magmas relies almost exclusively on whole rock major and trace element data. There is little information on isotopic variation among the Mesozoic basaltic rocks, and there are few high-quality age determinations. Here, we report Sr, Nd and Pb isotopic data for a single, compositionally zoned, Mesozoic diabase dike. The evidence for interaction with crustal rocks is distinct but subtle. Additionally, we document compositional variation that is expressed, across strike, as a dramatic increase in interstitial granophyre content. We focus on the implications of this compositional zoning for models of open vs. closed system evolution of diabase magmas.

Across-strike zoning occurs in numerous large diabase dikes, but relatively few studies document these variations (Ernst and others, 1987; Hermes, 1964; Ragland and others, 1968; Sol, 1987; Steele and Ragland, 1976). Numerous dikes of the Mackenzie swarm of northern

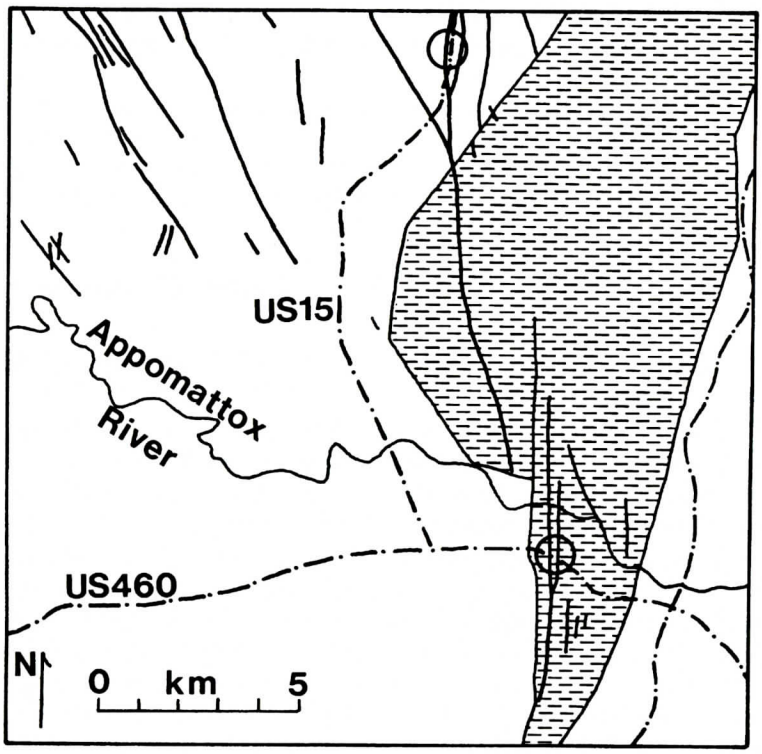

Figure 1. Geologic sketch map of the area near the Farmville dike. Diabase dikes are shown as solid lines. Sampling locations are circled. Dot-dash lines indicate major roadways. The city of Farmville is located north and east of the junction of US 460 and US 15. The fault-bounded Triassic Farmville Basin is shaded. Modified from Gottfried and others (1991).

Canada have granophyre-rich cores (Gibson and others, 1987; pers. comm., M. B. Lambert and T. D. Peterson); some dikes of the Sudbury swarm in southern Ontario are also zoned, but less dramatically (pers. comm., K. A. Bethune and A. Davidson). These dikes include mildly alkaline, ne-normative compositions, in addition to ol-normative and q-normative tholeiites. The processes responsible for generating compositional zoning potentially affect a broad range of basaltic magmas. In compositionally zoned sills and flows, gravity segregation combines with flow processes to produce both vertical and lateral change (Mangan and others, 1993; Philpotts and others, 1996; Steiner and others, 1992). A different model is needed to interpret compositional variation in vertical or near-vertical dikes because gravity segregation is unlikely to produce zoning across strike.

GEOLOGIC SETTING

This study focuses on a quartz tholeiitic diabase dike that is exposed near Farmville in south-central Virginia (Figure 1). Located within the Piedmont physiographic province, the dike trends N-S and cuts across the boundary fault of the Mesozoic Farmville basin. It can be traced, based on its aeromagnetic expression, through the western part of the Farmville Basin and into metamorphic basement rocks at least to 37°30'N (VDMR, 1970; James, 1991). Gottfried and others (1991) trace the dike and its en echelon segments for at least 15 km, and possibly for 23 km (connection between the main dike and the northernmost segment is not exposed at the surface). Geophysical data (VDMR, 1970; James, 1991), our mapping and the mapping of Gottfried and others (1991) all indicate that the dike is vertical to within 5°.

West of the Farmville Basin, the pre-Mesozoic stratigraphy is assigned to the Cambrian(?) Chopawamsic Fm. (Marr, 1980), which is dominated by amphibolite-grade biotite gneisses (metavolcanics) and ferruginous quartzites. The eastern margin of the basin abuts gneisses assigned to the Hatcher Complex (Brown, 1969) of Ordovician age (Mose, 1980). Within the basin, the dike cuts Triassic sedimentary rocks correlative with the Newark Supergroup.

Mesozoic diabase dikes in Virginia belong to two swarms that differ in orientation. Dikes that trend N-S are generally longer, wider, farther apart, and more variable in strike than dikes that trend NE (Milla and Ragland, 1992; Ragland, 1991; Ragland and others, 1983). The N-S dikes are compositionally evolved (i.e., SiO_2 > 51 wt.%, MgO < 6 wt.%) quartz tholeiites, whereas the NE dikes are generally less evolved. The Farmville dike belongs to the N-S swarm, as indicated by the mapping of Gottfried and others (1991).

No dating has been done on the N-S dikes in Virginia. Data for the Culpeper (197±4 Ma; $^{40}Ar/^{39}Ar$ incremental heating; Sutter and others, 1983) and Gettysburg (201±1 Ma; U/Pb on zircon; Dunning and Hodych, 1990) sills, which are also quartz tholeiitic, indicate that an age of 200±5 Ma is appropriate for the Farmville dike. N-S dikes in North Carolina also fall within this age range (Sutter, 1985, 1988, and unpublished data). Accumulating evidence indicates that almost all of the igneous activity associated with breakup of Pangaea occurred around 200±5 Ma (Marzoli and others, 1999).

Regionally, the diabases of eastern North America (ENA) comprise compositionally distinct groups of olivine and quartz tholeiites (Ragland and others, 1992). The olivine tholeiites are further divided into groups that are relatively enriched and depleted in incompatible elements, whereas the quartz tholeiites include high-titanium (HTQ), low-titanium (LTQ), and high-iron (HFQ) groups (Ragland and others, 1983). These compositional variants may represent different petrogenetic histories, and one goal of this study is to constrain the petrogenesis of the group to which the Farmville dike belongs. Granophyre, the micropegmatite of other authors, is a common accessory component in many of these diabases, but rarely exceeds 5 vol.%; the Farmville dike is exceptional in having a core zone in which granophyre exceeds 30 vol.%. Preliminary reports on the Farmville dike have been presented in Rogan and Dudás (1992), Rogan (1993), and Bounds and Dudás (1997).

SAMPLING AND ANALYSES

The Farmville dike was sampled in two locations (Figure 1). Highway US 460 cuts the dike near Farmville at a sharp angle so that the dike has an apparent width of about 400 m, and a true thickness of about 150 m. Along US 460, exposure is poor (about 30%), but some outcrop is accessible over almost the full width of the dike. Neither contact was located, but finer grained diabase, which we interpret to represent the chilled margin, occurs at both ends of the sampled transect. Rocks at the western limit of exposure are almost aphyric. Two to five kg. samples were taken approximately every three meters across the dike, as exposure allowed; the west side of the dike was more closely sampled. The first sample on the west serves as the zero point for all cross sections. At the second sampling location, along US 15, fresh diabase from a branch of the main dike was sampled for petrographic comparison with the US 460 samples. Here, the highway parallels the dike, and cross-strike sampling was not possible.

Thin sections were prepared from the freshest samples collected at each location. Point counts of plagioclase, pyroxene, granophyre and opaque abundances (300 to 400 points per section) were completed on a representative set of 32 sections from the US 460 location. Electron microprobe analyses of pyroxenes, plagioclase, and Fe-Ti oxides were done on an ETEC SA-3 microprobe, using 15 kV accelerating potential, 200 na beam current, and mineral standards supplied by the Smithsonian Institution.

A selection of 16 samples from the US 460 site was ground in an alumina shatterbox, and analyzed for major elements and some trace elements by induction coupled plasma spectrophotometry (ICP). The samples were prepared

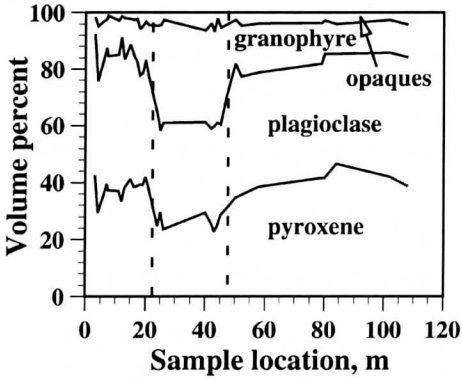

Figure 2. Modal compositions of samples from the US 460 site. Distance is measured from the location of the westernmost sample. Granophyre abundance increases, mostly at the expense of plagioclase, in the core of the dike.

Table 1: Selected plagioclase compositions

	US 460		US 15		
SiO_2	54.46	53.91	54.29	53.46	51.58
Al_2O_3	28.36	28.00	27.74	28.72	30.05
FeO	1.04	0.73	0.68	0.81	0.76
CaO	10.52	11.14	9.99	12.08	12.96
Na_2O	5.41	4.82	5.60	4.27	3.82
K_2O	0.36	0.28	0.39	0.26	0.23
Total	100.15	98.88	98.69	99.60	99.40
Or	2.1	1.7	2.3	1.5	1.4
Ab	47.2	43.2	49.2	38.4	34.3
An	50.7	55.2	48.5	60.1	64.3

Table 2. Selected pyroxene compositions

	Augite						Pigeonite			
	US 460			US 15			US 460	US 15		
SiO_2	48.60	47.54	49.51	52.05	48.40	48.43	50.27	50.43	50.12	48.72
TiO_2	0.75	0.59	0.36	0.42	0.66	0.53	0.35	0.43	0.48	0.45
Al_2O_3	1.52	2.73	0.71	1.64	1.27	2.27	0.83	0.78	0.86	0.92
FeO	19.75	24.28	21.60	13.64	22.69	16.30	28.32	29.90	29.55	28.27
MnO	0.45	0.53	0.86	0.32	0.49	0.40	0.67	0.65	0.69	0.65
MgO	12.04	9.31	6.16	14.80	10.05	11.49	16.80	13.02	12.86	13.85
CaO	15.92	15.10	21.36	17.37	14.59	19.15	4.02	5.28	5.79	5.38
Na_2O	0.18	0.25	0.17	0.19	0.16	0.19	0.04	0.07	0.07	0.05
Cr_2O_3	0.07	0.03	0.02	0.02	nd	0.04	nd	0.03	nd	0.03
Total	99.28	100.36	100.75	100.45	98.31	98.80	101.30	100.59	100.42	98.32
Wo	31.7	29.5	45.3	34.6	30.3	38.9	4.7	10.4	11.2	9.2
En	39.0	31.7	19.1	43.7	32.0	37.9	51.8	38.8	38.7	43.5
Fs	29.3	38.8	35.5	21.7	37.7	23.1	43.5	50.8	50.1	47.3
% nq	5.8	7.9	3.0	2.9	3.6	6.8	4.2	1.2	1.6	3.0
Average values										
	n = 14			n = 22			n = 18	n = 17		
Wo	35.65±4.77			32.39±4.38			9.19±2.64	10.14±2.02		
En	31.48±8.91			36.92±7.01			48.36±5.70	44.33±8.11		
Fs	32.87±6.09			30.69±8.28			42.46±5.55	45.54±8.07		
% nq	4.37±1.60			4.29±1.50			3.17±1.00	2.53±1.11		

% nq: mole % of non-quadrilateral components

by lithium metaborate fusion, using methods modified from Medlin and others (1969). Accuracy of the ICP data was monitored by analyses of up to 7 international rock standards, and precision was evaluated from 10 replicate analyses of USGS standard W2. Precision was better than accuracy, which was better than 2% (relative) for all major elements except Na_2O (2.3% rel.), and better than 5% (rel.) for all trace elements except Ba (9%), Zn (14%) and Y (26%). Isotopic analyses were completed following methods described in Walker and others (1994). All chemical analyses were done at the Carnegie Institution of Washington.

RESULTS

Field Observations, Petrography and Mineralogy

The dike appears to be a single intrusion. No internal contacts (i.e., chilled zones within the dike) were found, but may occur in covered intervals. The transition from granophyre-poor to granophyre-rich diabase occurs over less than 6 m, and may be much sharper; no change of grain size occurs in this interval. Throughout the dike, granophyre is uniformly dispersed, and does not occur as segregated zones. The bulk of the dike is medium grained, with average grain size between 1 and 2 mm, and has subophitic texture.

Results of modal analyses are plotted in Figure 2. Primary minerals are pyroxene, plagioclase, quartz, alkali feldspar, apatite and Fe-Ti oxides; trace amounts of sulfides and baddeleyite(?) also occur. Virtually all quartz and alkali feldspar occur in intimate, graphic intergrowths, shown as granophyre on Figure 2. Olivine and orthopyroxene are absent. Alteration products include chlorite, biotite, amphibole, epidote, white mica ("sericite"), carbonate, prehnite and Fe hydroxides ("limonite"). Amphibole and biotite may be late magmatic, rather than hydrothermal phases. Even the freshest samples contain at least 5 vol.% of alteration products, primarily as chlorite, biotite and amphibole replacing pyroxene, and sericite replacing feldspars. Alteration is related to hydrothermal effects near veins, and primarily to metasomatism near granophyre.

Plagioclase is the dominant mineral in the diabase. Numerous petrographic determinations (Michel-Levy and universal stage) indicate compositions between An_{58} and An_{75}, whereas electron microprobe analyses indicate plagioclase compositions between An_{33} and An_{65} (Table 1), with only few analyses below An_{48}.

The majority of plagioclases are labradorites, and most grains are not strongly zoned. Where present, zoning is normal, with a difference of <10 mol.% An between cores and rims. Microprobe analyses indicate about 1 wt.% FeO in plagioclase, presumably as ferric ions in the tetrahedral site. Intense alteration of plagioclase near K-feldspar bearing granophyre suggests disequilibrium between the feldspars. Two-feldspar thermometry is not possible for these rocks, both because the feldspars are not contemporaneous, and because virtually all alkali feldspar is strongly altered. Microprobe analysis of K-feldspar was precluded by alteration.

Augite and pigeonite were identified among the pyroxenes (Figure 3 and Table 2). Micro-

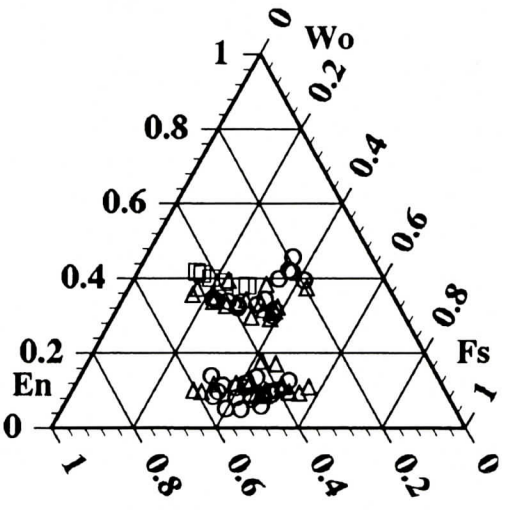

Figure 3. Pyroxene compositions recalculated into Wo-En-Fs components. Open triangles are from the US 15 site; open circles are from the US 460 site. Open squares are compositions predicted by COMAGMAT, with each point representing an increment of 10% solidification; pyroxene in equilibrium with the average dike composition is the most magnesian model point.

probe analyses indicate that about 40% of the pyroxene is pigeonite. Pigeonite is petrographically distinguishable from augite only where, due to orientation, it has higher refractive index than immediately adjacent augite. Textures suggest that plagioclase and both pyroxenes crystallized contemporaneously, though pigeonite commonly occurs in the cores of augite aggregates. Pyroxene compositions are similar at both sampling locations. Augite ranges from $Wo_{36}En_{50}Fs_{14}$ to $Wo_{30}En_{30}Fs_{40}$, and some grains are strongly zoned, with Fe-rich margins. Compositional variation in single grains suggests crystallization over a range of conditions. A second, Hd-rich pyroxene population occurs in samples from the US 460 location, and may have formed late in the history of the magma. Pigeonite compositions evolve from relatively Mg-rich (En_{60}) to relatively Fe-rich (Fs_{58}), and are variable in CaO content (4 - 12 mol.% Wo). Pigeonite is less strongly zoned than augite. Pyroxenes contain less than 8 mol.% of non-quadrilateral components.

In most samples, granophyre is the third most abundant constituent. Its modal distribution is strikingly non-uniform across the width of the dike (Figure 2). In the bulk of the dike, granophyre occupies 6 - 20 vol.%, and is distributed as interstitial patches of variable size and irregular shape. In the core of the dike, it constitutes 30 - 37 vol.%, always as interstitial, dispersed patches that post-date plagioclase and pyroxene. Apatite needles are abundant in the granophyre. Granophyre patches average 300 μm, with average quartz grain sizes between 20 - 50 μm; the largest granophyre patches are near 2 mm in diameter. Near granophyre, most plagioclase and pyroxene are altered, suggesting that granophyre represents quenching of a hydrous melt during the latest stages of solidification of the magma.

Fe-Ti oxides constitute 1 - 6 vol.% of the dike. Both magnetite and ilmenite were originally present; virtually all magnetite has been oxidized and altered, whereas ilmenite remains relatively fresh. Iron oxide thermometry is precluded by alteration of magnetite. The Fe-Ti oxides generally formed late in the paragenesis, and are typically interstitial to plagioclase and pyroxene, though rare oxide grains are included in pyroxene. The mostly subhedral, primary oxide grains range up to 1 mm in size, but average 200 μm.

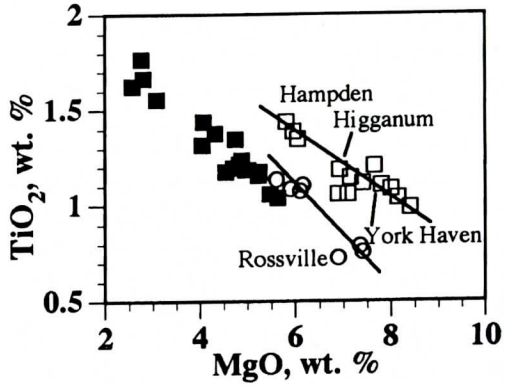

Figure 4. MgO-TiO_2 plot of data from the Farmville dike (filled squares), compared with other Mesozoic diabases from eastern North America. Open circles and squares are for incompatible element depleted and enriched diabase, respectively. Plot and trend lines from Puffer and Philpotts (1988).

Geochemistry: Major and Trace Elements

Representative chemical analyses are presented in Table 3. The Farmville dike is a quartz normative tholeiite, and belongs to the HFQ group of Ragland and others (1992). The SiO_2 content of the dike averages 53 wt.% (54.8 wt.% on an anhydrous basis), and is high, compared with most other ENA diabases. MgO content (average 4.8 wt.%, or 5.0 wt.% on an anhydrous basis) is slightly lower than that of other HFQ diabases (Figure 4), and decreases toward the core of the dike. Figure 4 indicates that the Farmville dike is on the fractionated end of the trend defined by incompatible-element depleted, high-Fe diabases (Puffer and Philpotts, 1988). Mg-number is low (< 50) and mafic index is high (> 54). In the core of the dike, particularly, the TiO_2 content is well above that in other HFQ diabases. Compositional variation of the dike (Figures 5 and 6) is compatible with patterns expected from frac-

Table 3. Chemical compositions and modes of selected samples from the Farmville Dike, Virginia

	FV-15	FV-22	FV-36	FV-38	FV-40	FV-47	Main Dike	Granophyre
Major Elements, wt.%							Average	Average
SiO_2	53.90	52.50	58.40	56.00	52.50	53.10	52.95±0.51	57.33±1.22
TiO_2	1.03	1.21	1.62	1.66	1.31	1.23	1.23±0.11	1.68±0.07
Al_2O_3	13.90	13.00	13.20	12.40	12.80	13.30	13.01±0.51	12.63±0.49
FeO	10.30	10.60	10.10	10.20	10.10	10.60	10.44±0.19	10.17±0.06
Fe_2O_3*	2.01	2.07	1.98	2.00	1.98	2.09	2.05±0.04	2.00±0.02
MnO	0.22	0.21	0.18	0.18	0.19	0.21	0.21±0.01	0.18±0.00
MgO	5.62	4.80	2.55	2.79	4.03	4.86	4.80±0.48	2.70±0.13
CaO	9.75	8.85	6.48	5.70	8.33	8.96	8.96±0.45	6.09±0.39
Na_2O	2.36	2.16	2.93	3.00	2.07	2.21	2.22±0.11	2.97±0.04
K_2O	0.56	0.70	2.26	2.07	0.69	0.70	0.69±0.05	2.10±0.15
Total	99.65	96.10	99.70	96.00	94.00	97.26	96.56	97.85
Trace Elements, ppm								
Zr	82	91	165	167	110	98	107±16	160±7
Sr	153	145	142	128	147	154	147±5	138±7
Y	25	28	45	46	32	32	29.6±3.8	44.4±1.5
Zn	93	105	118	122	107	105	114±19	117±4
Cu	40	47	61	64	56	46	52.2±7.8	66.0±7.9
Sc	50	45	38	41	43	49	49.1±3.1	39.6±1.5
Ni	18	11	nd	nd	16	11	9.58±5.11	3.2±6.6
Cr	23	14	nd	nd	8	13	13.4±4.2	5.2±5.9
V	384	369	339	375	373	402	397±17	351±16
Ba	135	178	325	323	225	178	178±25	329±33
Mode, vol.%								
plagioclase	47.9	38.5	37.1	31.8	47.3	43.8	44.7±4.5	35.1±3.8
pyroxene	37.0	39.3	22.7	28.5	24.5	42.0	38.6±3.6	26.6±3.0
granophyre	12.3	16.3	33.5	34.5	15.5	11.5	13.5±3.5	33.9±3.9
opaques	2.8	6.0	6.1	5.1	3.0	2.7	3.2±1.2	4.5±1.5

* Calculated as 0.15 total Fe, atomic.

tional crystallization: the granophyric core of the dike is enriched in incompatible elements (SiO_2, TiO_2, Na_2O, K_2O, Ba, and Zr) and depleted in compatible elements (MgO, CaO, Ni and Cr). Variation exceeds analytical uncertainty for most elements, but is undetectable for Al_2O_3, Fe (t) and Sr. The extent of enrichment in the core is remarkable, ranging up to a factor of three for K_2O.

In the absence of unaltered samples, it is impossible to assess the effect of alteration on the bulk rock chemistry. The distribution of elements that are mobile during low grade hydrothermal alteration (SiO_2, CaO, Na_2O, K_2O, Rb, Ba, Sr, Pb), and particularly of those that are concentrated in feldspars, may reflect hydrothermal rather than primary igneous processes. Prehnite bearing veins occur locally within the dike and demonstrate hydrothermal element mobility.

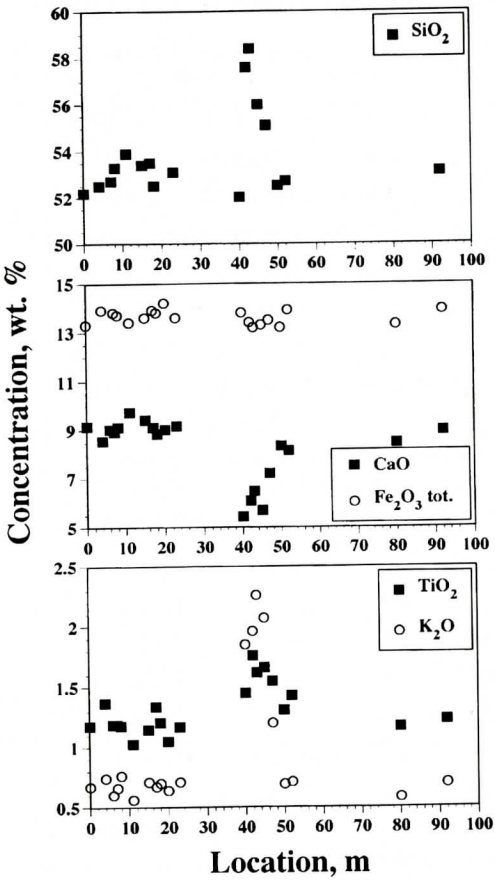

Figure 5. Compositional variation across the Farmville dike. Most elements show dramatic changes between the diabase and the granophyric core, but a few, like Fe_2O_3 (t), do not.

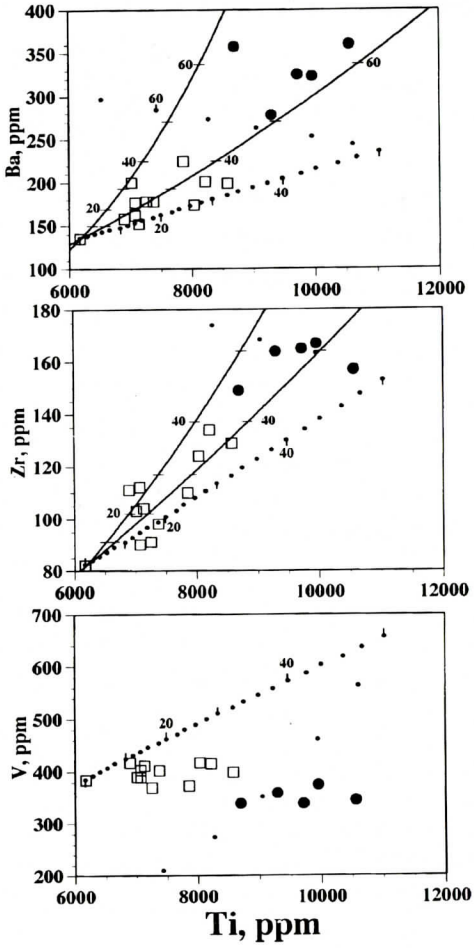

Figure 6. Trace element covariation diagrams for the Farmville dike and model predictions. Filled circles are granophyre-rich samples. Solid lines show simple Rayleigh fractionation models; COMAGMAT trends are shown as points, each representing 2% solidification. Tick marks indicate 10% solidification increments. Bulk distribution coefficients for Rayleigh models are: D_{Ba} = 0.001; D_{Ti} = 0.4 and 0.7 (for Ti-Ba); D_{Zr} = 0.001; D_{Ti} = 0.3 and 0.5 (for Ti-Zr).

Geochemistry: Isotopic Compositions

Bulk rock Nd, Sr and Pb isotopic compositions are reported in Table 4. In these samples, the Sr and Pb isotopic systems could be disturbed because of feldspar alteration, and Nd isotopic data are considered most reliable. Excluding the core of the dike, age-corrected ε_{Nd} is between -1 and -2.5 and $^{87}Sr/^{86}Sr$ is between 0.705 and 0.707 (Figure 7); present-day $^{206}Pb/^{204}Pb$ is between 18.9 and 19 (Figure 8). For all three isotopic systems, the granophyric core samples are distinct from the bulk of the dike: ε_{Nd} and Pb isotopic ratios are lower (Figure 9), whereas $^{87}Sr/^{86}Sr$ is higher. The differences, for all isotopic systems, are greater than analytical uncertainty.

These isotopic compositions are similar to those previously reported for ENA diabases (Pegram, 1990; Ragland and others, 1998). The Farmville dike plots with quartz-normative diabases from the northern part of the ENA province (Figs. 8), not with compositions of dikes in North and South Carolina, most of which are

Table 4. Isotopic data for the Farmville Dike.

	FV-15	FV-22	FV-36	FV-38	FV-40	FV-47
Rb, ppm	17.93		91.67	83.30	28.38	50.79
Sr, ppm	144.3	144.9	136.8	125.4	143.5	145.5
$^{87}Rb/^{86}Sr$	0.364		1.962	1.945	0.579	1.022
$^{87}Sr/^{86}Sr$	0.70776	0.70821	0.71304	0.71300	0.70848	0.70813
$^{87}Sr/^{86}Sr(i)$	0.70673		0.70746	0.70747	0.70684	0.70522
Sm, ppm	2.93	3.68	5.56	5.79	4.27	3.72
Nd, ppm	11.12	14.56	22.89	23.64	16.77	14.21
$^{147}Sm/^{144}Nd$	0.1591	0.1530	0.1468	0.1479	0.1540	0.1584
$^{143}Nd/^{144}Nd$	0.512475	0.512522	0.512386	0.512404	0.512456	0.512525
$^{143}Nd/^{144}Nd(i)$	0.512267	0.512322	0.512194	0.512210	0.512254	0.512318
ε at 200 Ma	-2.17	-1.10	-3.59	-3.27	-2.41	-1.18
$^{206}Pb/^{204}Pb$	18.952	18.924	18.700	18.648		18.953
$^{207}Pb/^{204}Pb$	15.676	15.668	15.645	15.637		15.664
$^{208}Pb/^{204}Pb$	38.901	38.886	38.725	38.656		38.883

(i) indicates calculated initial value at 200 Ma.
Sr isotopic compositions are reported relative to 0.71025 for NBS987; Pb isotopic compositions are reported relative to the NBS981 values of Todt and others (1996); Nd isotopic compositions are normalized to $^{146}Nd/^{144}Nd = 0.7219$, and reported relative to 0.511850 for LaJolla Nd. Blanks are estimated to be 100 pg, 10 pg and 20 pg for Sr, Nd and Pb, respectively.

olivine diabases.

DISCUSSION

Petrographic and geochemical data indicate significant variation across the strike of the Farmville dike. To a first approximation, models for interpreting such compositional variations and for forming granophyre are composites of three "end-members" that appeal to chemical differentiation (Walker, 1940), physical, fluid dynamic processes (Mangan and others, 1993; Philpotts and others, 1996), or contamination and assimilation (Marsh, 1989; Philpotts and Asher, 1993; Stewart and DePaolo, 1990) as the dominant mechanism. Chemical differentiation models assume that compositional variation results from closed system crystallization processes that affect a single volume of magma, and that, therefore, granophyre is a geochemical derivative of the enclosing diabase. Physical models emphasize gravitational instability and fluid dynamic properties, mostly coupled with fractional crystallization, to account for the spatial distribution of chemically distinct units within individual intrusions. Contamination - assimilation models account for some of the compositional variation by linking crystallization with assimilation of melts from surrounding wall rocks, either at the site of intrusion or at some point along the transport path of the magmas. Research supporting these models focuses mostly on sills (e.g., the Palisades) and lopoliths (e.g., Skaergaard), where horizontal layering is prominent, and gravity segregation is a possible mechanism of separating solids and melts. In vertical dikes, gravity segregation is unlikely to

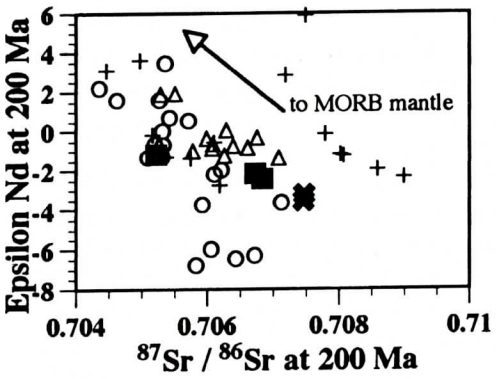

Figure 7. Nd-Sr isotopic covariation diagram for initial isotopic ratios of the Farmville dike and other eastern North American tholeiites. Filled squares are for Farmville diabase; crosses are for Farmville granophyre; open circles are North and South Carolina diabases (Pegram, 1990); open triangles are for diabases from the northern part of the ENA province (Pegram, 1990); and crosses are other ENA diabases from Pe-Piper and others (1992) and Puffer (1992).

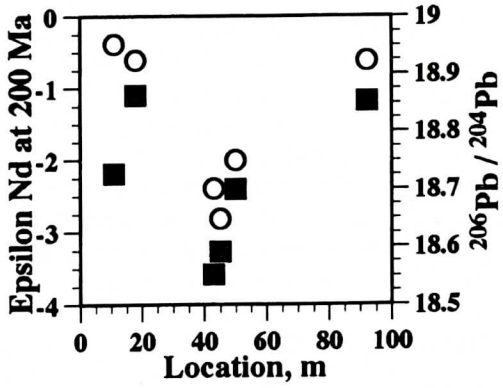

Figure 9. Spatial variation of initial Nd (filled squares) and present-day Pb (open circles) isotopic ratios across the Farmville dike. Values in the granophyric core are lower than those in the bulk of the dike.

produce compositional variation across strike.

Most recent models invoke multiple processes. Mangan and others (1993), from detailed study of the high-Ti quartz tholeiite of the York Haven sheet in south-central Pennsylvania, conclude that fractional crystallization, flow differentiation and closed-system hydrothermal transport were important. The maximum SiO_2 and K_2O contents of York Haven samples are 54.07 and 1.21 wt.%, well below those observed in the Farmville dike; at the same time, TiO_2 content reaches a maximum of 3.35 wt.%, almost twice that of the Farmville dike. Philpotts and others (1996) develop a mush-compaction model to interpret the distribution of pegmatitic segregations in the quartz-tholeiitic Holyoke basalt flow in Connecticut. These segregations are clearly intrusive, and most formed from melts that were extracted from the bulk magma after about 33% crystallization. They interpret smaller, granophyric segregations as immiscible melts formed after over 70% crystallization. Steiner and others (1992) review evidence and models for compositional variation in the Palisades sill, another high-Ti quartz tholeiite, and propose a cumulus-transport-deposition (CTD) model, combined with multiple intrusion, to explain the data. Some granophyre-rich samples of the Palisades sill reach over 57 wt.% SiO_2, but the CTD model does not extend to this silicic range. Thus, none of these studies presents a model that plausibly explains the Farmville data, at least in part because they depend on gravitational segregation in subhorizontal sheets to generate granophyre-enriched horizons. Unconstrained by isotopic data, they do not evaluate the potential contribu-

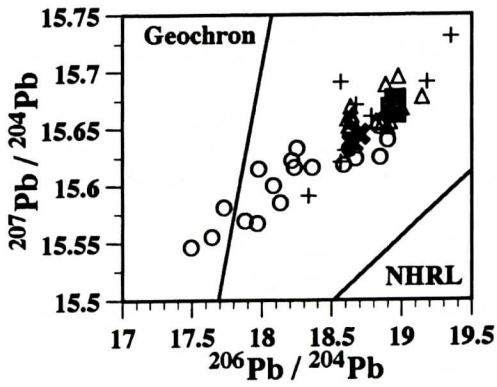

Figure 8. Lead isotopic data for the Farmville dike and other eastern North American tholeiites. Symbols and data sources as in Figure 7. NHRL: northern hemisphere regression line of Hart (1984).

tion of crustal melts.

Some studies clearly implicate assimilation. Puffer and Benimoff (1997) document fractionation, hydrothermal alteration and local wall-rock assimilation at Laurel Hill, New Jersey, where compositions include low-Ti quartz tholeiite, high-Ti quartz tholeiite and high-Fe quartz tholeiite. Their preferred model derives all rock types from a high-Ti quartz tholeiite parent magma. They consider assimilation reactions to have occurred at the site of intrusion. Husch and Schwimmer (1985) document selective, local contamination in the Quarry dike near New Hope, Pennsylvania. In a review of diabases from the central Newark basin, however, Husch (1992) concludes that "residual granophyric compositions were produced by ~70 - 80% total crystallization and they exhibit no geochemical evidence for being the result of large-scale crustal anatexis," but the minimum age-corrected $^{87}Sr/^{86}Sr$ he reports is 0.70575, above the minimum value of 0.70522 observed in the Farmville dike. Philpotts and Asher (1993) document assimilation reactions in the Higganum dike and overlying Talcott basalt in Massachusetts and Connecticut. They demonstrate that assimilation occurred locally along dike contacts, that anatectic melts mixed into the magma during intrusion, and that wall-rock reactions potentially occurred over a vertical distance of > 10 km, contaminating the whole volume of the magmatic system.

Three constraints derive from cursory examination of the Farmville dike data, and indicate that no simple model can account for its zoning. The first is that intrusion occurred under turbulent flow conditions. The width of the dike, and the absence of (observed) internal contacts, is consistent with turbulent conditions. The dispersed distribution of granophyre suggests that the interior of the dike was well-mixed: granophyre is not the product of a crystallization front, or of a gravitationally segregated residual melt. Both within the dike and the granophyric core, granophyre is mixed with the other constituents, and never forms continuous zones or pods. The inference of turbulent conditions during intrusion rests critically on the assumption that magma was actively flowing through a dike width ≥ 10 meters. It is likely that magma was not actively flowing through the whole width of the dike at any one time, and that the present width of the dike results either from a sustained, continuous fissure eruption, or from multiple intrusion.

A second constraint is that the granophyric core of the dike, by mass balance, could not result from fractional crystallization of the magma volume presently preserved in the dike. The proportion of granophyre is greater than the amount that could be produced in a closed system, if that system is defined as the dike itself. If closed system fractionation were the mechanism responsible for compositional variation, the fractionation process would have occurred in an underlying magma chamber. The granophyric core would then represent either a second intrusion or a magma volume that, during protracted tapping of the magma chamber, sampled a significantly more fractionated magma volume.

The third constraint is that isotopic differences between the granophyric core and the rest of the dike demonstrate that the magma system was open to components derived from at least two isotopically distinct sources: closed system processes are inadequate to describe the evolution of the dike magma.

Major and Trace Element Data and Fractionation Models

Much of the major and trace element data mimics closed system processes, and, if these were the only data available, we could conclude that closed system processes, under a range of conditions, generated the Farmville dike. We used the COMAGMAT model (Ariskin and others, 1993), with no assimilation, to test closed system behavior. COMAGMAT calculates crystallization paths from experimentally determined saturation surfaces in singly- or multiply-saturated systems; it calculates both phase compositions and residual magma compositions as a function of temperature (percent of crystallization). The model calculates trace element concentrations by adjusting bulk distribution coefficients to match the crystallizing

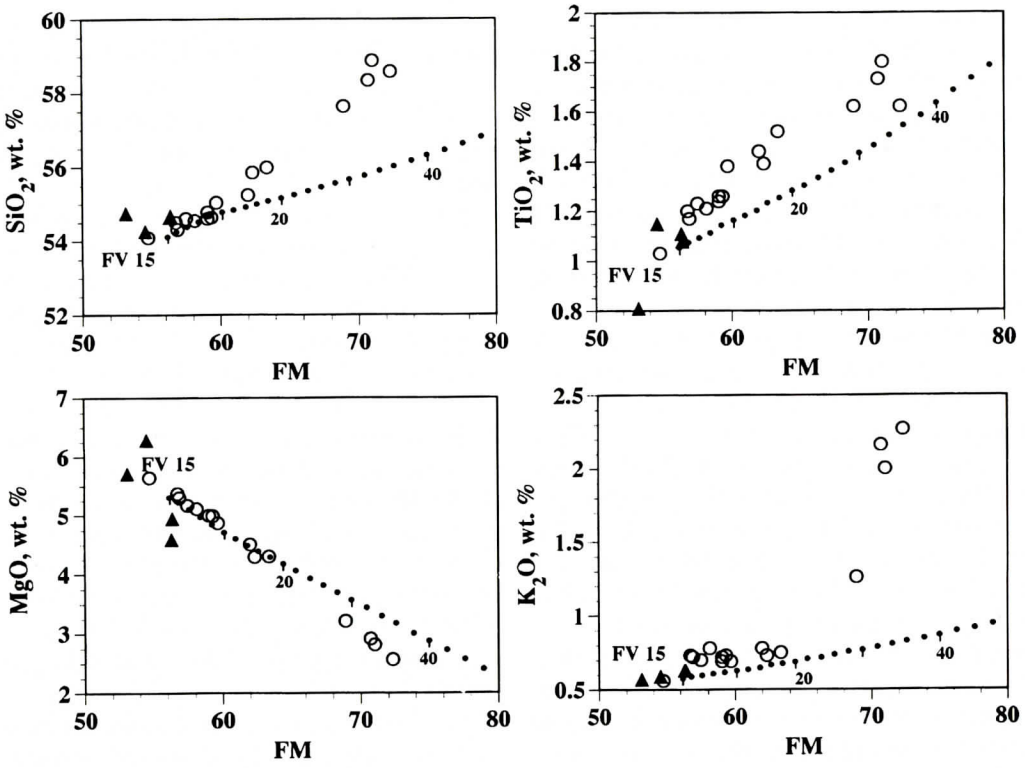

Figure 10. Element variation plotted against the femic index (atomic Fe total / (Mg + Fe total)*100), a measure of differentiation. Data for the Farmville dike (open circles) are plotted along with calculated trends from the COMAGMAT model. Solid triangles show fractionation of 10% augite, pigeonite, and plagioclase, and 1% ilmenite. K_2O and SiO_2 are very poorly predicted by fractionation models.

phase assemblage and the temperature. To examine the range of possible fractionation paths, we tested both the average dike composition (excluding the granophyric core) and the most magnesian sample (FV 15) as starting compositions for modeling, recognizing that the latter may contain cumulus pyroxene. We assumed atmospheric pressure because there is no constraint on the depth of crystallization; that the average Farmville dike composition plots near the multiply-saturated 1 atm. cotectic (c.f., Yang and others, 1996) is permissive evidence of low pressure crystallization. Oxygen fugacity for the COMAGMAT calculation was set at the quartz-fayalite-magnetite buffer, though variation of ± 2 log units from the buffer did not materially affect model results.

For most major and trace elements, COMAGMAT yields residual magma compositions that are remarkably close to observed rock compositions (e.g., MgO in Figure 10), particularly for the main part of the dike. COMAGMAT indicates that fractional crystallization of 40% of the magma could account for variation of most major elements, but model results differ from the data for SiO_2, TiO_2, and K_2O. At least 50% fractionation is needed to match incompatible trace element concentrations (Figure 6), and data for Ba, Zr and V are not compatible with model results. Several of these (SiO_2, K_2O, Ba, V) are components that can be mobilized during hydrothermal alteration or evolution of a hydrothermal fluid from a magma. In the absence of isotopic data, there is no compelling evidence for processes other than fractionation and alteration, as Husch (1992), Houghton and others (1992) and other researchers have concluded. Fractional crystallization is obviously an important control on compositional variation.

Approximately linear covariation patterns, such as shown in Figure 10 for SiO_2, TiO_2 and MgO, can result from fractionation or from binary mixing processes. The femic index, in addition to being a differentiation index, can also be regarded as a proxy for modal granophyre content. These approximately linear correlations suggest both fractionation and mixing (open system) processes could have contributed to compositional variation.

The elevated TiO_2 content of the granophyric core is problematic. In closed system models, crystallization of ilmenite and spinel-structured oxides must be suppressed to yield high TiO_2 in residual magmas. In most COMAGMAT models, either spinel or ilmenite begins crystallizing after 40 - 50% solidification, when TiO_2 content is similar to that of the granophyre, but the femic index of model melts exceeds that of the granophyre (Figure 10). COMAGMAT also predicts that V content should increase with fractionation, but the opposite is observed (Fig. 6), and Ti-V covariation in the dike is difficult to explain. Because V is strongly fractionated into magnetite, and magnetite is almost completely altered in the dike, the Ti-V covariation may result from alteration reactions.

There are two additional discrepancies between the data and COMAGMAT results. Olivine is absent from the Farmville dike, whereas it is the first phase to crystallize in the model, and, under virtually all model conditions, constitutes 5 - 10 wt.% of the solid assemblage. The pyroxene compositions predicted by COMAGMAT are not compatible with observations; model augites are significantly more calcic (Figure 3), and pigeonite is only rarely crystallized in the models, whereas it constitutes about 40% of the pyroxene assemblage in the dike. The bulk composition of the dike plots very close to the plagioclase+magnetite saturated augite-pigeonite cotectic at 1 atm., but COMAGMAT model compositions plot within the augite stability field. Considering the range of results produced by different modeling approaches (Yang and others, 1996), these discrepancies alone are insufficient to dismiss closed system fractionation as the dominant process. Similar discrepancies in fractionation models are reported by Hough-

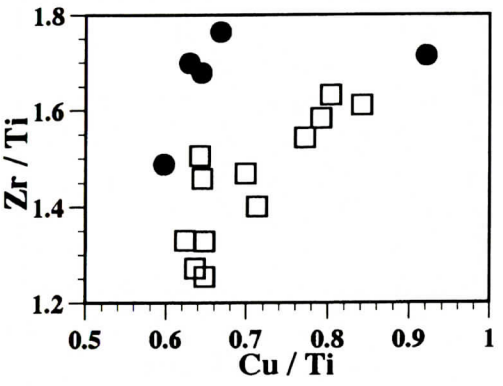

Figure 11. A plot of Cu against Zr, both normalized to Ti, suggests that hydrothermal alteration cannot account for the distribution of elements in the Farmville dike. Filled circles show data from the granophyre-rich portion of the dike.

ton and others (1992), who accommodate the elevated TiO_2 content of the residual magma by adding over 9% magnetite and ilmenite from an unspecified source to their fractionation model, yet conclude that assimilation is not consistent with trace element data and heat balance considerations. Our isotopic data and the discrepancy in TiO_2 demonstrate that closed system processes, though important, are inadequate to explain compositional variation in the Farmville dike.

In the York Haven diabase, Mangan and others (1993) ascribe elevated TiO_2 content in ferrogabbro to hydrothermal processes within the magma system. Unlike the Farmville dike, TiO_2 variation in the ferrogabbro is not coupled with large excursions in SiO_2 and K_2O content. To test whether hydrothermal effects might have modified compositions in the Farmville Dike, we plotted Cu/Ti against Zr/Ti (Fig. 11). In principle, Cu should be highly mobile in the hydrothermal environment, whereas Zr and Ti should be relatively immobile, so that high Cu/Ti should be associated with hydrothermally altered rocks. Most samples from the granophyric core have Cu/Ti values comparable to the lowest values observed in the dike, and hydrothermal effects are therefore unlikely to account for variation in TiO_2.

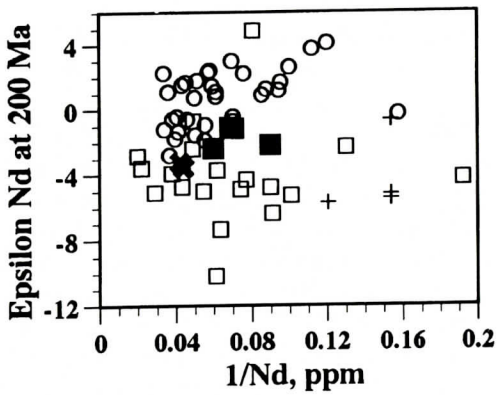

Figure 12. Initial Nd isotopic composition of the Farmville dike (filled symbols; squares are for the main part of the dike) plotted against inverse Nd concentration. Small crosses are diabase data from Pegram (1990). Isotopic compositions from potential contaminant sources in the Carolina Terrane (open circles; Samson and others, 1995; Wortman and others, 1996) and the Milton Belt (open squares; Wortman and others, 1996) are shown for comparison.

Isotopic Data: Evidence for Open System Processes

Most components that are poorly matched by fractionation models are strongly affected during assimilation of crustal melts. Isotopic differences between the granophyre-rich core and the main mass of the Farmville dike could result from assimilation, or from modification, during hydrothermal alteration, of parent - daughter ratios: Nd and Sr isotopic compositions are more radiogenic and Pb compositions less radiogenic in the granophyre. During hydrothermal alteration, because Rb is more mobile than Sr, and K-feldspar more strongly altered than plagioclase, Rb/Sr would be decreased in the more strongly altered granophyric portion of the dike. The data, however, show higher Rb/Sr in the granophyric portion of the dike. Isotopic compositions also show that this elevated Rb/Sr is not an artifact of processes that post-date intrusion: even at 200 Ma, the Sr isotopic composition of the granophyric core of the dike is more radiogenic. A similar argument can be made for the Pb isotopic data; the stronger alteration of relatively Pb-rich K-feldspars should increase U/Pb in the granophyric portion of the dike, whereas the data show that Pb compositions in the granophyre are less radiogenic. In systems showing low grade hydrothermal alteration, rare earth element mobility is unlikely, and the differences in rare earth element concentrations and Nd isotopic compositions must reflect original features of the magmatic system. Isotopic data, thus, reflect magmatic rather than hydrothermal processes.

Compared to the diabase magma, the isotopic contaminant had higher Rb/Sr and lower Sm/Nd and U/Pb. These relative element abundances are consistent with those expected in anatectic melts from middle or upper crustal rocks. In particular, the Nd concentrations and isotopic compositions of some Milton Belt schists and gneisses (Figure 12; Wortman and others, 1996) are similar to those expected for the contaminant. This suggests the hypothesis that anatexis of amphibolite-grade metamorphic rocks (e.g., the Hatcher complex) produced the isotopic contaminant. The majority of diabase dikes in North and South Carolina have Nd isotopic compositions $\varepsilon_{Nd,200} < -1$ (Pegram, 1990), and despite their magnesian compositions, as Ragland and others (1998) recognized, Pegram's conclusion that they have not been contaminated by interaction with crustal melts is unwarranted. In particular, detection of contamination from analyses of single samples is difficult. Similarly, the conclusion of Husch (1992) that there is no evidence of crustal assimilation in the diabases of the Newark basin is open to question, in view of the elevated Sr isotopic compositions of several of his samples.

As indicated by the range of isotopic compositions in the granophyre-poor part of the dike, the bulk of the dike also may contain variable percentages of this contaminant. From the limited data, the isotopic composition of uncontaminated diabase magma cannot be estimated with any certainty, nor can the percentages of "basalt" and contaminant be estimated. Philpotts and Asher (1993) conclude, based on mass balance arguments using major elements, that contamination in excess of 6 wt.% is likely for the quartz-normative Talcott basalt and its feeder, the Higganum dike, in which grano-

phyre is only a minor constituent.

Unlike the case of the Higganum dike, where exposure allowed sampling of the dike and its contacts over a vertical range, vertical sampling is not possible for the Farmville dike, and there is no indication of where assimilation or contamination of the magma occurred. The dispersal of granophyre throughout the dike suggests that the fractionation and assimilation reactions occurred at some distance from the sampled exposures.

Models for Petrogenesis of the Farmville Dike

Two models are potentially consistent with the available data. If, as the absence of internal contacts suggests, the Farmville dike was formed by sustained, continuous magma transport through a gradually widening fissure, the remarkable change in granophyre content toward the core of the dike must represent a change, as a function of progressive intrusion, in magma composition in the source. This model assumes that there is a geochemical relation between the main mass of the dike and its granophyric core, an assumption that is reasonable in view of the data we have. The parental magma, which is not represented at the present level of exposure, underwent fractionation and contamination in a crustal magma chamber prior to intrusion. Anatexis of biotite-bearing rocks similar to amphibolites of the Milton Belt produced hydrous, buoyant, essentially granitic melt that potentially draped the top of the magma chamber, and may have mixed with the basaltic magma. During intrusion, varying proportions of this felsic melt were entrained and mixed with the diabase magma; there was only limited miscibility between the magmas because of density and viscosity contrasts. Mixing produced dispersed granophyre in the main mass of the dike, as well as chemical patterns that are almost indistinguishable from those of fractional crystallization. The core of the dike contains a greater proportion of granitic melt, potentially sampled from the top of the magma chamber as the supply of hot basaltic magma waned. Crystallization of the granophyre (mostly hydrous anatectic melt) released high temperature hydrothermal fluids that altered the dike.

The compositional contrast between the main mass of the dike and its granophyric core could also be due to multiple intrusion, and multiple intrusion is the simplest explanation of the data. In a multiple intrusion model, the granophyre in the main mass of the dike would be produced by fractionation of the dike magma itself, and the granophyre-rich core would represent either a completely unrelated intrusion of relatively felsic magma, or a batch of strongly fractionated and contaminated diabase magma. Post-magmatic alteration, again, would reflect release of hydrothermal fluids during crystallization of the granophyre.

Variants of a multiple intrusion model may differ from the mixing and continuous intrusion model only in a semantic sense, because the latest, granophyre-rich portion of the dike is compositionally distinct from the main mass of the dike, and could be considered at least a separate intrusive episode. Under turbulent flow conditions, there is no mechanism for concentrating felsic, residual melt in the core of the dike, and a change in the composition of the intruded magma is the only possible explanation.

There are two observations that may be incompatible with the continuous intrusion model. One is the anomalous behavior of TiO_2, and the other is that the granophyre-rich core, based on our mapping, is not centrally located within the dike. In a continuous intrusion model, the latest intrusive phase would probably be centrally located.

Several aspects of the multiple intrusion model are problematic. If granophyre in the main mass of the dike is derived from fractional crystallization of the dike magma, this fractionation process could not have occurred in-situ, in the dike itself. The granophyric melt does not appear to be in equilibrium with minerals crystallizing from the diabase magma. The uniform distribution of granophyre in the main mass of the dike indicates that melt and solids were not separated, which is what fractionation requires. In diabase sills of similar composition, a comparable volume of dispersed granophyre does

not develop during in-situ crystallization. Even in a multiple intrusion model, there is a need to explain the uniform distribution of granophyre in the main mass of the dike. Though much of the exposure is covered, there is no evidence of chilled zones within the dike, which would be diagnostic of multiple intrusion. In multiple intrusion models, the origin of the magma in the granophyre-rich core of the dike is open to a range of interpretations, and is not necessarily causally linked with evolution of the diabase. The data, however, suggest a chemical relation between the main mass of the dike and the granophyric core; multiple intrusion models do not require such a relationship. There is no evidence, regionally, of magmas having compositions similar to the core of the dike. Stoddard (1992) documents early Mesozoic silicic dikes in northern North Carolina, but none of these is compositionally similar to the core of the Farmville dike. Furthermore, mixing between diabase and magmas similar to Stoddard's could not produce the composition of the core.

No model adequately explains TiO_2 variation. Anatectic melts equilibrated with residual Fe-Ti oxides usually have low TiO_2 content; only if residual Fe-Ti oxides were absent would these melts have TiO_2 content similar to that of the granophyre. Assimilation of Ti-rich anorthosite (such as the Roseland anorthosite in Nelson Co., VA), might produce melts with elevated TiO_2 content. Usually, TiO_2 is immobile during hydrothermal alteration, and transport occurs only when hydrothermal fluids are rich in CO_2 (Murphy and Hynes, 1986). We therefore consider hydrothermal enrichment of TiO_2 unlikely. Because some Fe-Ti oxides crystallized with pyroxenes and plagioclase in the Farmville dike, we consider TiO_2 enrichment by fractional crystallization, alone, insufficient, though there is no question that fractional crystallization was important. In our view, this TiO_2 enigma is the least tractable aspect of interpreting the petrogenesis of the Farmville dike.

CONCLUSIONS

The Farmville dike is a high-Ti quartz tholeiite. It extends for at least 15 km, is 150 m. wide, and has a 30-m thick granophyre-rich core. Modal abundance of granophyre averages 15 vol.% in the main mass of the dike, and 35 vol.% in the granophyric core. The bulk of the dike has SiO_2 content near 53 wt.%, whereas the granophyric core reaches 58 wt.% SiO_2. The Nd, Sr and Pb isotopic compositions of the core differ from those of the main mass of the dike, and indicate that open system processes are partly responsible for the cross-strike zoning of the dike.

Closed system modeling, using COMAGMAT, closely approximates major element variation in the main mass of the dike, but cannot reproduce SiO_2, K_2O, TiO_2 and Ba concentrations in the core. Phase compositions and assemblages calculated by COMAGMAT are also at variance with those observed, but the close approximation of model results to major element patterns in the main mass of the dike indicates that fractional crystallization was an important control on compositional variation. Isotopic variations indicate that the Farmville magma was contaminated by a component containing higher Rb/Sr and lower Sm/Nd and U/Pb than the parental diabase. These characteristics are consistent with contamination by a hydrous anatectic melt formed at mid-crustal levels. Some rocks of the Milton Belt in North Carolina have isotopic compositions appropriate to the contaminant, and biotite gneisses of the Hatcher Complex, exposed to the east of the Triassic Farmville Basin, are potential sources of the contaminant.

Fractional crystallization, contamination, magma mixing and hydrothermal alteration combined to produce the zoning observed in the Farmville dike. Fractional crystallization accounts for most of the major element distributions; contamination is required to explain isotopic variations; magma mixing or multiple intrusion is required to account for the spatial distribution of compositionally distinct parts of the dike; and hydrothermal alteration redistributed mobile elements. We cannot exclude multiple intrusion, but there is no evidence supporting multiple intrusion in preference to magma mixing during continuous intrusion.

Our research suggests that, in the absence of

isotopic data, crustal contamination would not have been detected. Other studies of Mesozoic diabases potentially have overlooked a significant source of compositional variation because they lack isotopic constraints.

ACKNOWLEDGMENTS

Part of this study was completed by PTR for his MS thesis at Old Dominion University. We thank the Geological Sciences Program at ODU for its support. J. Beard of the Virginia Museum of Natural History (Martinsville) guided early stages of PTR's work, and B. Waller and D.T. Hurdle assisted PTR in the field. The Department of Terrestrial Magnetism of the Carnegie Institution of Washington (R.W. Carlson and S.B. Shirey) provided facilities for chemical and isotopic analyses. Isotopic analyses were supported by Tark Geosciences. W.J. Bounds, with help from S. Marshall, collected some of the microprobe data. We also thank P.C. Ragland of Florida State University for his insights in evaluating some of our early results, and Ragland and A. R. Philpotts for helpful reviews.

REFERENCES CITED

Ariskin, A. A., Frenkel, M. Ya., Barmina, G. S., and Nielsen, R. L., 1993, COMAGMAT: A FORTRAN program to model magma differentiation processes: Computers & Geosciences, v. 19, p. 1155-1170.

Bounds, W. J., and Dudás, F. Ö., 1997, Compositions of pyroxene and plagioclase in the Mesozoic Farmville diabase dike: Virginia Journal of Science, v. 48, p. 123.

Brown, W. R., 1969, Geology of the Dillwyn Quadrangle, Virginia: Virginia Division of Mineral Resources Report of Investigations 10, 77 pp.

Dunning, G. R., and Hodych, J. P., 1990, U/Pb zircon and baddeleyite ages for the Palisades and Gettysburg sills of the northeastern United States: Implications for the age of the Triassic / Jurassic boundary: Geology, v. 18, p. 795-798.

Ernst, R. E., Bell, K., Ranalli, G., and Halls, H. C., 1987, The Great Abitibi dyke, southeastern Superior Province, Canada, in Halls, H. C., and Fahrig, W. F., eds., Mafic Dyke Swarms: Geological Association of Canada Special Paper 34, p. 123-135.

Froehlich, A. J., and Robinson, G. R., Jr., 1988, Studies of the Early Mesozoic Basins of the Eastern United States: U.S. Geological Survey Bulletin 1776, 423 pp.

Gibson, I. L., Sinha, M. N., and Fahrig, W. G., 1987, The geochemistry of the Mackenzie dyke swarm, Canada, in Halls, H. C., and Fahrig, W. F., eds., Mafic Dyke Swarms: Geological Association of Canada Special Paper 34, p. 109-121.

Gottfried, D., Froehlich, A. J., and Grossman, J. N., 1991, Geochemical data for Jurassic diabase associated with early Mesozoic basins in the eastern United States: U. S. Geological Survey Open File Report OF 91-0322.

Hart, S. R., 1984, A large-scale isotope anomaly in the Southern Hemisphere mantle: Nature, v. 309, p. 753-757.

Hermes, O. D., 1964, A quantitative petrographic study of dolerite in the Deep River Basin, North Carolina: American Mineralogist, v. 49, p. 1718-1729.

Houghton, H. F., Herman, G. C., and Volkert, R. A., 1992, Igneous rocks of the Flemington fault zone, central Newark basin, New Jersey: Geochemistry, structure, and stratigraphy: in Puffer, J. H., and Ragland, P. C., eds., Eastern North American Mesozoic Magmatism: Geological Society of America Special Paper 268, p. 219-232.

Husch, J. M., 1992, Geochemistry and petrogenesis of the Early Jurassic diabase from the central Newark basin of New Jersey and Pennsylvania: in Puffer, J. H., and Ragland, P. C., eds., Eastern North American Mesozoic Magmatism: Geological Society of America Special Paper 268, p. 169-192.

Husch, J. M., and Schwimmer, R. A., 1985, Major and trace element concentrations across a Mesozoic basaltic dike, New Hope, Pennsylvania: Northeastern Geology, v. 7, p. 144-160.

James, C. G., Jr., 1991, A Geophysical and Geological Study of the Farmville Triassic Basin: unpublished M. S. thesis, Old Dominion University, Norfolk, 186 pp.

Mangan, M. T., Marsh, B. D., Froehlich, A. J., and Gottfried, D., 1993, Emplacement and differentiation of the York Haven diabase sheet, Pennsylvania: Journal of Petrology, v. 34, p. 1271-1302.

Marr, J. D., Jr., 1980, The geology of the Willis Mountain quadrangle, Virginia: Virginia Division of Mineral Resources Publication 25, scale 1:24,000.

Marsh, J. S., 1989, Geochemical constraints on coupled assimilation and fractional crystallization involving upper crustal compositions and continental tholeiitic magma: Earth and Planetary Science Letters, v. 92, p. 70-80.

Marzoli, A., Renne, P. R., Piccirillo, E. M., Ernesto, M., Bellieni, G., and De Min, A., 1999, Extensive 200-million-year-old continental flood basalts of the central Atlantic magmatic province: Science, v. 284, p. 616-618.

Medlin, J. H., Suhr, N. H., and Bodkin, J. B., 1969, Atomic absorption analyses of silicates employing $LiBO_2$ fusion: Atomic Absorption Newsletter, v. 8, p. 25 - 29.

Milla, K. A., and Ragland, P. C., 1992, Early Mesozoic Talbotton diabase dikes in west-central Georgia: Compositionally homogeneous high-Fe quartz tholeiites, in Puffer, J. H., and Ragland, P. C., eds., Eastern North American Mesozoic Magmatism: Geological Society of America Special Paper 268, p. 347-359.

Mose, D. G., 1980, Rb-Sr whole-rock studies: Virginia Pied-

mont, II: Carnegie Institution of Washington Yearbook, p. 483-485.

Murphy, J. B., and Hynes, A. J., 1986, Contrasting secondary mobility of Ti, P, Zr, Nb and Y in two metabasaltic suites in the Appalachians: Canadian Journal of Earth Sciences, v. 23, p. 1138-1144.

Pegram, W. J., 1990, Development of continental lithospheric mantle as reflected in the chemistry of Mesozoic Appalachian tholeiites, U.S.A.: Earth and Planetary Science Letters, v. 97, p. 316-331.

Pe-Piper, G., Jansa, L. F., and Lambert, R. St. J., 1992, Early Mesozoic magmatism on the eastern Canadian margin: Petrogenetic and tectonic significance, *in* Puffer, J. H., and Ragland, P. C., eds., Eastern North American Mesozoic Magmatism: Geological Society of America Special Paper 268, p. 13-36.

Philpotts, A. R., and Asher, P. M., 1993, Wallrock melting and reaction effects along the Higganum diabase dike in Connecticut: Contamination of a continental flood basalt feeder: Journal of Petrology, v. 34, p. 1029-1058.

Philpotts, A. R., Carroll, M., and Hill, J. M., 1996, Crystal-mush compaction and the origin of pegmatitic segregation sheets in a thick flood-basalt flow in the Mesozoic Hartford Basin, Connecticut: Journal of Petrology, v. 37, p. 811-836.

Puffer, J. H., 1992, Eastern North American flood basalts in the context of the incipient breakup of Pangaea, in Puffer, J. H., and Ragland, P. C., eds., Eastern North American Mesozoic Magmatism: Geological Society of America Special Paper 268, p. 95-118.

Puffer, J. H., and Benimoff, A. I., 1997, Fractionation, hydrothermal alteration, and wall-rock contamination of an Early Jurassic diabase intrusion: Laurel Hill, New Jersey: Journal of Geology, v. 105, p. 99-110.

Puffer, J. H., and Philpotts, A. R., 1988, Eastern North American quartz tholeiites: Geochemistry and petrology, *in* Manspeizer, W., ed., Triassic-Jurassic Rifting: Continental Breakup and the Origin of the Atlantic Ocean and Passive Margins: Developments in Geotectonics 22, Elsevier, New York, p. 579-605.

Puffer, J. H., and Ragland, P. C., 1992, Eastern North American Mesozoic Magmatism: Geological Society of America Special Paper 268, 400 pp.

Ragland, P. C., 1991, Mesozoic igneous rocks, in Horton, J. W., and Zullo, V. A., eds., The Geology of the Carolinas: University of Tennessee Press, p. 171-190.

Ragland, P. C., Cummins, L. E., and Arthur, J. D., 1992, Compositional patterns for early Mesozoic diabases from South Carolina to Virginia, in Puffer, J. H., and Ragland, P. C., eds., Eastern North American Mesozoic Magmatism: Geological Society of America Special Paper 268, p. 309-331.

Ragland, P. C., Hatcher, R. D., Jr., and Whittington, D., 1983, Juxtaposed Mesozoic diabase dike sets from the Carolinas: A preliminary assessment: Geology, v. 11, p. 394-399.

Ragland, P. C., Kish, S. A., and Parker, W. C., 1998, Compositional patterns for Lower Mesozoic olivine tholeiitic diabase dikes in the Deep River Basin, North Carolina: Southeastern Geology, v. 38, p. 91-102.

Ragland, P. C., Rogers, J. J. W., and Justus, P. S., 1968, Origin and differentiation of Triassic dolerite magmas, North Carolina, USA: Contributions to Mineralogy and Petrology, v. 57, p. 305-316.

Rogan, P. T., 1993, Petrology of a large, granophyre-rich Mesozoic diabase dike near Farmville, Virginia: unpublished M. S. thesis, Old Dominion University, Norfolk, 112 pp.

Rogan, P. T., and Dudás, F. Ö., 1992, Petrology of a large, granophyre-rich Mesozoic diabase dike near Farmville, Virginia: Geological Society of America Abstracts with Programs, v. 24, p. 61.

Samson, S. D., Hibbard, J. P., and Wortman, G. L., 1995, Nd isotopic evidence for juvenile crust in the Carolina terrane, southern Appalachians: Contributions to Mineralogy and Petrology, v. 121, p. 171-184.

Sol, A., 1987, Chemical and petrographic variations across transverse profiles of four early Mesozoic diabase dikes from North Carolina: unpublished M. S. thesis, Florida State University, Tallahassee, 207 pp.

Steele, K. F., and Ragland, P. C., 1976, Model for the closed-system fractionation of a dike formed by two pulses of dolerite magma: Contributions to Mineralogy and Petrology, v. 57, p. 305-316.

Steiner, J. C., Walker, R. J., Warner, R. D., and Olson, T. R., 1992, A cumulus - transport - deposition model for the differentiation of the Palisades sill, in Puffer, J. H., and Ragland, P. C., eds., Eastern North American Mesozoic Magmatism: Geological Society of America Special Paper 268, p. 193-217.

Stewart, B. H., and DePaolo, D. J., 1990, Isotopic studies of processes in mafic magma chambers: II. The Skaergaard intrusion, east Greenland: Contributions to Mineralogy and Petrology, v. 104, p. 125-141.

Stoddard, E. F., 1992, A new suite of post-orogenic dikes in the eastern North Carolina Piedmont: Part II. Mineralogy and geochemistry: Southeastern Geology, v. 32, p. 119-142.

Sutter, J. F., 1985, Progress on geochronology of Mesozoic diabases and basalts: in Robinson, G. P., and Froehlich, A. J., eds., Proceedings of the second U. S. Geological Survey conference on the early Mesozoic basins of the Eastern United States, U. S. Geological Survey Circular 946, p. 110-114.

Sutter, J. F., 1988, Innovative approaches to the dating of igneous events in the early Mesozoic basins of the eastern United States: *in* Froehlich, A. J., and Robinson, G. P., Jr., eds., Studies of the Early Mesozoic Basins of the Eastern United States, U. S. Geological Survey Bulletin 1776, p. 194-199.

Sutter, J. F., Arth, J. G., and Leavy, J. G., 1983, $^{40}Ar/^{39}Ar$ age spectrum dating and strontium isotope geochemistry of diabase sills from the Culpeper Basin, Virginia: Geological Society of America, Southeastern Section, 32nd Annual Meeting, Abstracts with Programs, p. 92.

Todt, W., Cliff, R. A., Hanser, A., and Hofmann, A. W.,

1996, Evaluation of a ^{202}Pb - ^{205}Pb double spike for high precision lead isotope analysis, *in* Basu, A., and Hart, S. R., eds., Earth Processes: Reading the Isotope Code: American Geophysical Union Geophysical Monograph 95, p. 429-437.

Virginia Division of Mineral Resources, 1970, Aeromagnetic contour map of the Farmville quadrangle: Open File report, scale 1:62,500.

Walker, F., 1940, Differentiation of the Palisades diabase, New Jersey: Geological Society of America Bulletin, v. 51, p. 1059-1106.

Walker, R. J., Carlson, R. W., Shirey, S. B., and Boyd, F. R., 1994, Os, Sr, Nd and Pb isotope systematics of southern African peridotite xenoliths: Implications for the chemical evolution of subcontinental mantle: Geochimica et Cosmochimica Acta, v. 53, p. 1583-1595.

Wortman, G. L., Samson, S. D., and Hibbard, J. P., 1996, Discrimination of the Milton Belt and the Carolina terrane in the southern Appalachians: A Nd isotopic approach: Journal of Geology, v. 104, p. 239-247.

Yang, H.-J., Kinzler, R. J., and Grove, T. L., 1996, Experiments and models of anhydrous, basaltic olivine-plagioclase-augite saturated melts from 0.001 to 10 kbar: Contributions to Mineralogy and Petrology, v. 124, p. 1-18.

SOUTHEASTERN GEOLOGY
V. 39, No. 1, November 1999, p. .37-50

DOCUMENTING LATE PROTERZOIC RIFTING IN THE OCOEE BASIN, WESTERN BLUE RIDGE, NORTH CAROLINA

CAMILO MONTES

Department of Geological Sciences, University of Tennessee, Knoxville, TN 37996

ROBERT D. HATCHER, JR.

Department of Geological Sciences, University of Tennessee, Knoxville, TN 37996, and Environmental Sciences Division, Oak Ridge National Laboratory, Oak Ridge, TN 37831

ABSTRACT

Detailed geologic mapping in the western Blue Ridge of western North Carolina indicates that the Snowbird Group-Great Smoky Group contact is the premetamorphic Greenbrier fault. Redefinition of this contact confines the entire Snowbird Group to the footwall of the Greenbrier fault. Reinterpretation of this boundary demands an alternative explanation for large thickness changes of Snowbird strata (from more than 1,000 m to less than 200 m) in the Cataloochee Divide area previously explained by telescoping along the Greenbrier fault. A northeast-trending, northwest-dipping normal fault active during the accumulation of the Longarm Quartzite also explains these changes, and agrees well with the tectonic setting of the Ocoee Supergroup along the extending Late Proterozoic rifted margin of Laurentia. This fault limited the eastward extent of the Ocoee basin, and probably hindered west-to-east sediment dispersal along the rifted margin of Laurentia.

INTRODUCTION

Although it is widely accepted that the Ocoee Supergroup accumulated in a rift basin along the eastern margin of Laurentia during the Late Proterozoic (Rodgers, 1972; DeWindt, 1975; Rankin, 1975; Rast and Kohles, 1986; Hatcher, 1989), no rift-related faults have previously been mapped in this clastic sequence or in the underlying Middle Proterozoic basement. Growth faults have been documented elsewhere in the Appalachian orogen by mapping stratigraphic contrasts of units accumulating during active crustal extension (Schwab, 1976; Wehr and Glover, 1985; Thomas, 1991). The basal unit of the Ocoee Supergroup (Snowbird Group) is the best candidate in the western Blue Ridge to record extension in the form of stratigraphic thickness contrasts. Indeed, in the easternmost western Blue Ridge, Hadley and Goldsmith (1963) mapped dramatic stratigraphic thickness changes in the Snowbird Group in the Cataloochee Divide area (Figure 1). They interpreted these changes, however, as the result of 24 km of westward thrusting along the pre-Taconic Greenbrier fault, which placed thin, proximal sequences and underlying basement (formerly located at the eastern edge of the basin) onto more distal, thicker sequences of the Snowbird Group. This paper redefines the Snowbird Group-Great Smoky Group contact in the easternmost western Blue Ridge as the easternmost extension of the Greenbrier fault. Redefinition of this contact confines the entire Snowbird Group to the footwall of the Greenbrier fault. Thus, we postulate that changes in Snowbird Group stratigraphy in the easternmost western Blue Ridge record Late Proterozoic rifting and coeval sedimentation. Geological relationships supporting this hypothesis are based on the results of detailed field mapping in the eastern flank of the Great Smoky Mountains of western North Carolina.

Our detailed field mapping (1:24,000 scale; Montes, 1997) focused on the crosscutting relationships between the Longarm Quartzite and the units above (Great Smoky Group), and below it (granitic basement), in the Dellwood and

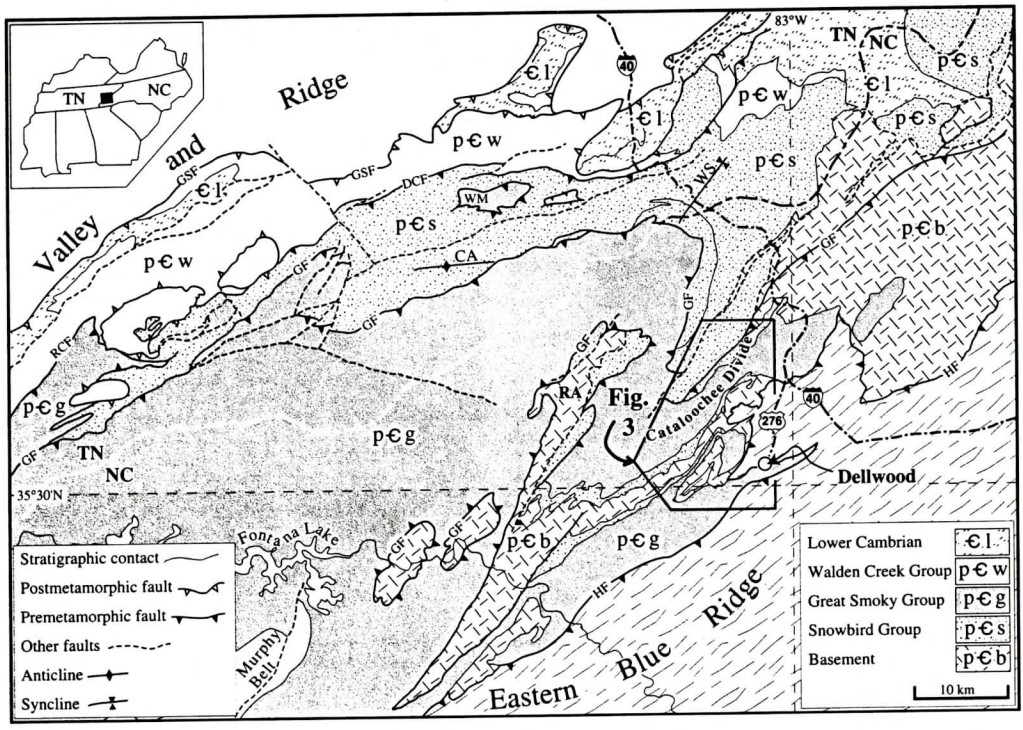

Figure 1. Geologic map of the western Blue Ridge showing the original trace of Greenbrier fault by King and others (1958), updated after Woodward and others (1991), Connelly and Woodward (1992), Carter and others (1995a), Carter and others (1995b). Other contacts and faults in North Carolina and northeastern Tennessee from Hardeman (1966), North Carolina Geological Survey (1985), Rast and Kohles (1986), and Hatcher (1989). CA: Copeland anticline; DCF: Dunn Creek fault; GF: Greenbrier fault; GSF: Great Smoky fault; HF: Hayesville fault; RA: Ravensfort anticline; RCF: Rabbit Creek fault; WM: Webb Mountain; WS: Waterville syncline.

parts of Bunches Bald, Cove Creek Gap, Sylva North, and Hazelwood 7 1/2 minute quadrangles. Detailed mapping consisted of walking out contacts, following marker beds or distinctive lithologic types, describing mineral assemblages, and collecting structural and stratigraphic data. These data allowed us to map structural truncations, assemble composite stratigraphic sections, and draw isograds. Exposures near Cataloochee Divide (Figure 1) yielded the most useful stratigraphic information because deformation is relatively simple here. To the southeast, both intense deformation, and higher metamorphic grade, made the study of stratigraphic units more difficult. The stratigraphic columns and thickness values we present in this paper are the result of calculation of stratigraphic thicknesses from outcrop widths on the geologic map, and correction of apparent thicknesses using dip data. Composite stratigraphic sections were assembled from individual outcrops in places where deformation was too severe to preserve a complete section. Down-plunge projection of structural data was used to construct the cross section presented in this paper. In order to measure changes in sandstone composition across the area mapped, and to compare earlier modes by Hadley and Goldsmith (1963), point counting was performed on 17 sandstone samples assuming that metamorphism was isochemical.

GEOLOGIC SETTING

The western Blue Ridge of North Carolina and Tennessee is part of a polydeformed crystalline thrust sheet emplaced westward onto platform sequences of the eastern margin of

Table 1. Stratigraphic nomenclature of the Ocoee Supergroup modified from King and others (1968), and Carter and others (1995b). The contact redefined in this paper (the Snowbird Group-Great Smoky Group contact) is highlighted with a thick line.

AGE	North and below Greenbrier fault	South and above Greenbrier fault
Early Cambrian	Chilhowee Group	Murphy belt rocks / Nantahala Slate and higher units
		conformable?
Late Proterozoic	Ocoee Supergroup: Walden Creek Group; Unclassified formations; Snowbird Group	Ocoee Supergroup: Great Smoky Group: Dean Formation; Ammons Formation; Anakeesta Formation; Thunderhead Sandstone; Elkmont Sandstone
		conformable ?
		Snowbird Group: Roaring Fork Sandstone; Longarm Quartzite; Wading Branch Formation
		Nonconformity
Middle Proterozoic	Ortho- and paragneiss basement	Ortho- and paragneiss basement

Laurentia during the late Paleozoic Alleghanian orogeny. This crystalline thrust sheet, the Blue Ridge-Piedmont thrust sheet (Hatcher and others, 1989), is composed of distal Laurentian (eastern Blue Ridge and Piedmont) and Laurentian rifted-margin assemblages (western Blue Ridge). The internal metamorphic core of the Appalachians in the Piedmont terrane represents distal outer slope and rise assemblages, along with fragments of oceanic crust (Hatcher, 1989). The western Blue Ridge contains Grenville basement (Fullagar and others, 1997) and cover sequences (Ocoee Supergroup) that represent the rifted Laurentian margin following breakup of the supercontinent of Rodinia (Hoffman, 1991), and opening of the Iapetus ocean (Odom and Fullagar, 1984; Goldberg and others, 1986; Su and others, 1994) during the Late Proterozoic.

Ocoee Supergroup rocks record multiple deformation events. Peak metamorphism in the western Blue Ridge has been dated at 480 Ma using $^{40}Ar/^{39}Ar$ (Dallmeyer, 1975); 440-460 Ma using $^{40}Ar/^{39}Ar$ (Connelly and Dallmeyer, 1993); 466 Ma using U-Pb (Quinn and Wright, 1993); and farther east, in the eastern Blue Ridge at 495 Ma using high-resolution ion microprobe dating (Miller and others, 1998). Therefore, premetamorphic deformation fabrics in the western Blue Ridge, including isoclinal folding (Butler, 1973), and the Greenbrier fault, are likely to be early Taconic (Penobscottian?), and brittle postmetamorphic deformation fabrics can be correlated with the Alleghanian orogeny. The central and eastern portions of the western Blue Ridge were deformed and metamorphosed to middle to upper amphibolite facies (Carpenter, 1970; Abbott and Raymond, 1984) during the Taconic orogeny, and then transported westward in a crystalline thrust sheet onto the platform of Laurentia during the Alleghanian orogeny (Hatcher, 1989; Adams and Su, 1996).

The Ocoee Supergroup

The Ocoee Supergroup is a mostly clastic succession of immature, poorly sorted sandstone, conglomerate, and siltstone approximately 10 km thick (King and others, 1958; Rast and Kohles, 1986). Primary sedimentary textures in this stratigraphic succession reflect accumulation in a rifted continental environment (Rankin, 1975). The Ocoee Supergroup

rests on Grenville basement and is overlain by the Lower Cambrian Chilhowee Group. Traditionally, the Ocoee Supergroup has been subdivided according to its relative position with respect to the Greenbrier fault (Table 1): either north and below, or south and above the fault. Correlation among the three main units of the Ocoee Supergroup (Walden Creek Group, Great Smoky Group, and Snowbird Group) across major tectonic boundaries is often ambiguous because lateral as well as vertical relationships are not entirely clear (King and others, 1958; DeWindt, 1975; Rast and Kohles, 1986). It is clear, however, that the Snowbird Group is the oldest of the three subdivisions because it rests beneath the Walden Creek Group and nonconformably on Grenville basement. Similarly, the Walden Creek Group is the youngest unit because it is overlain by Lower Cambrian rocks in the western Great Smoky Mountains. Geologic mapping in the westernmost western Blue Ridge (Costello and Hatcher, 1991; Carter and others, 1995a; Carter and others, 1995b) has shown the contact between the Walden Creek Group and the Great Smoky Group in southeastern Tennessee and adjacent North Carolina is conformable, therefore supporting an intermediate position for this unit.

The Snowbird Group in the easternmost part of the western Blue Ridge consists of three units from top to bottom: Roaring Fork Sandstone, Longarm Quartzite, and Wading Branch Formation. Contrasting depositional environments have been interpreted for the Wading Branch Formation and the Longarm Quartzite. Keller (1980) suggested that the impure, poorly sorted nature of the Wading Branch Formation indicates continental accumulation, perhaps in quiet coastal lagoons intermittently affected by currents bringing coarser clastics into an otherwise pelitic sequence. The absence of granitic fragments and the paucity of feldspar with respect to quartz were interpreted by Hadley and Goldsmith (1963) as evidence of slow erosion, deep chemical weathering, and reworking of granitic basement before filling the discontinuous depressions. In contrast, sedimentary structures in the Longarm Quartzite record strong currents in braided fluvial systems (Keller, 1980) to fluviodeltaic environments (DeWindt, 1975). Its high feldspar content is an indication of rapid mechanical disintegration of the source rock with virtually no chemical decomposition (Hadley and Goldsmith, 1963; Hadley, 1970), which requires significant relief in the source area during deposition (Keller, 1980).

Thickness of the Snowbird Group southeast of the Cataloochee Divide sharply decreases to only one tenth of its thickness to the northwest (King and others, 1958). Farther southeast the Snowbird Group continues to gradually thin until it disappears. King and others (1958) and Hadley and Goldsmith (1963) interpreted the abrupt thinning of the Snowbird Group in the Cataloochee Divide region as a result of 24 km of westward displacement along the Greenbrier fault. Telescoping along this fault would have placed thin, proximal sequences of the Snowbird Group onto thicker, more distal sequences to the west, concealing intermediate sequences. A stratigraphic taper angle of about 3.5 degrees is assumed in order to postulate 24 km of displacement. The gradual thinning of the Snowbird Group farther east (in the hanging wall) was interpreted as onlap of a transgressive sequence toward the southeastern edge of the basin (Hadley and Goldsmith, 1963).

In the area mapped in this study (Montes, 1997), only the Wading Branch Formation, Longarm Quartzite, and Thunderhead Sandstone are well exposed (including top and bottom contacts); thus, we narrow our focus to those three units.

Wading Branch Formation

The Wading Branch Formation is a commonly thin and discontinuous unit that nonconformably overlies Middle Proterozoic quartz diorite orthogneiss. This unit is generally less than 100 m thick, and consists of highly variable impure, poorly sorted, sandy black metasiltstone, quartz-rich metaconglomerate, and impure, medium-grained, often conglomeratic metasandstone. The relative proportions of quartz and feldspar place the psammitic rocks from this unit within the subarkose to muddy subarkosic field in a Q-F-M diagram (Hadley and Goldsmith, 1963). The Wading Branch Formation

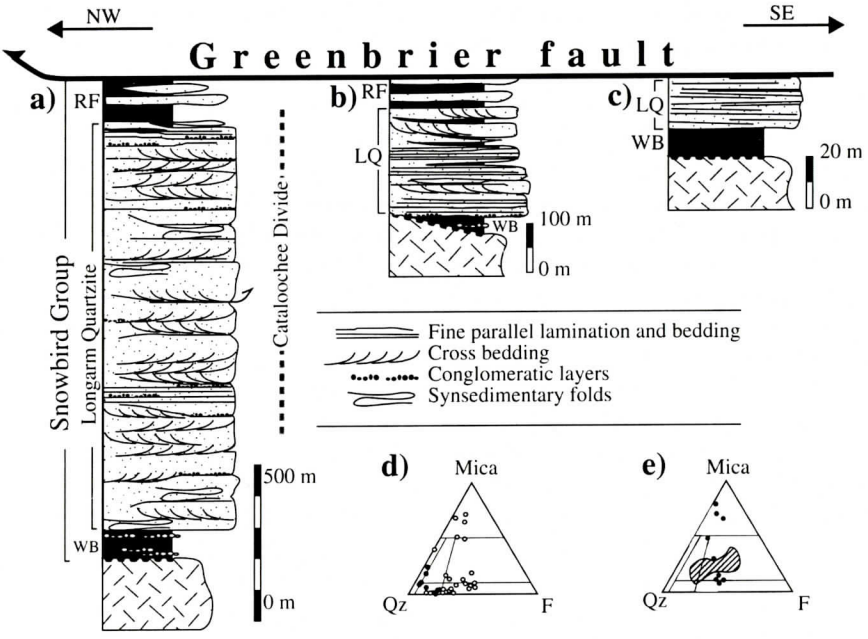

Figure 2. Simplified composite stratigraphic columns for the Snowbird Group. Note that vertical scale changes for every column. a) Northwest of Cataloochee Divide the Longarm Quartzite is a very thick, arkosic sandstone, containing abundant sedimentary structures. This section is exposed along the road to Cataloochee (from 35°38′15″ N, 83°3′41″ W to 35°38′13″ N, 83°5′1″ W). b) Southeast of the Cataloochee Divide the Longarm Quartzite is subarkosic and thinner. Cross bedding is still present. This section is exposed in the vicinity of Moody Top (from 35°32′33″ N, 83°5′11″ W to 35°33′5″ N, 83°5′32″ W). c) Farther southeast it consists of a very thin pelitic quartzite (35°31′12″ N, 83°4′53″ W). LQ: Longarm Quartzite; RF: Roaring Fork Sandstone; WB: Wading Branch Formation. d) Variation in composition across Cataloochee Divide. White dots are samples to the northwest (Hadley and Goldsmith, 1963), and black dots are samples to the southeast. e) Composition of the Thunderhead Sandstone in the area mapped (black dots), modal analyses by Hadley and Goldsmith (1963) in gray, and modal analyses by Quinn (1991) are dashed.

thins southeastward to less than 20 m near Dellwood, North Carolina. The basal contact of this unit is a nonconformity with granitic orthogneiss beneath.

Longarm Quartzite

The Longarm Quartzite is the most distinctive unit within the Snowbird Group because it is composed mostly of light-colored, very resistant, feldspathic sandstone. Northwest of Cataloochee Divide, the Longarm Quartzite consists of approximately 1,000 m of coarse- to medium-grained sandstone (Figure 2a). These deposits are characteristically arkosic to subarkosic, in 25 to 50 cm thick internally cross-bedded parallel beds, commonly containing soft-sediment slump folds. A rather abrupt decrease in thickness occurs east of Cataloochee Divide to a 50 to 200 m-thick unit of light-colored, commonly gray, fine-grained, biotite-rich subarkose with some pelite interlayers, and with conglomerate layers toward the base (Figure 2b). This subarkosic metasandstone gradually thins to the southeast where it pinches out into very fine-grained, muscovite-rich, pelitic quartzite to quartzite (Figure 2c). The basal contact of the Longarm Quartzite is either sharp and conformable with the Wading Branch Formation (Hadley and Goldsmith, 1963; Keller, 1980), or it is nonconformable on granitic basement.

Great Smoky Group

Rocks of the Great Smoky Group (Thunder-

head Sandstone and Elkmont Sandstone) compose the hanging wall of the Greenbrier fault in western North Carolina. Distinctive lithologic types within the Thunderhead Sandstone facilitated mapping of individual beds near its basal contact, and helped track premetamorphic faults by documenting tectonic truncations. The Thunderhead Sandstone in this area is an approximately 1200-m thick sequence of graded, fining-upward metaconglomerate-metasandstone-schist. Near the base it consists of 1- to 10-m thick intercalation of graded granule-size conglomerate beds with clasts of quartz, feldspar, and minor black siltstone, grading upward into fine-grained metasandstone. The contacts at the base of the coarse-grained units are always sharp with finer-grained units. Higher in this unit these conglomerate-sandstone beds gradually become graded, medium-grained, massive metasandstone that change upwards to fine-grained, laminated metasandstone, and finally to a sandy pelitic schist near the top of the unit. In general, the Thunderhead Sandstone near Dellwood is a coarse-grained unit near its base and to the northwest. Toward the top of the unit, and to the southeast, the Thunderhead Sandstone is a finer-grained more homogeneous unit. The same grain-size gradient was observed by Hadley and Goldsmith (1963) to the northwest. The contact with the underlying Elkmont Sandstone is transitional over a stratigraphic distance of 10 to 20 m. The Elkmont Sandstone unit in the area mapped in this study is a black, massive, and monotonous metasiltstone approximately 1,000 m thick. Occasional 1- to 3- m thick graded conglomeratic metasandstone beds break the monotony of this sequence. The base of the Elkmont Sandstone is faulted against the Caldwell and Greenbrier faults everywhere in the area mapped.

Greenbrier Fault

One of the major structures slicing the Ocoee Supergroup in the western Blue Ridge is the Greenbrier fault. It was originally mapped as a thrust fault separating the Snowbird Group from the Great Smoky Group (King and others, 1958). This fault does not offset isograds or affect the dominant foliation, and therefore predates metamorphism (King and others, 1958). The premetamorphic timing of the Greenbrier fault is further constrained by garnet-biotite geothermometry (Milton, 1983). According to Hadley and Goldsmith (1963) and Keller (1980), this fault was preceded by folding both in the hanging wall and in the footwall (in the Copeland Creek anticline and in the Waterville syncline), although Woodward and others (1991), interpreted these folds as a folded footwall ramp.

Mylonites have been reported along the trace of Greenbrier fault (Connelly and Woodward, 1992), but the main criterion traditionally used by early mappers (King and others, 1958; Hadley and Goldsmith, 1963) to map the Greenbrier fault is the lithologic contrast between fine-grained rocks from the top of the Snowbird Group in the footwall, and coarser-grained conglomerate and sandstone of the Great Smoky Group in the hanging wall. In the Cataloochee Divide area, however, Hadley and Goldsmith (1963) mapped the Greenbrier fault as a NNE-trending, steeply dipping fault juxtaposing Ocoee Supergroup rocks and basement to the east, and Snowbird Group rocks to the west. This mapped trace implies that the hanging wall ramp where the Greenbrier fault ramps up from basement is located in this region, because it is the easternmost basement exposure in the western Blue Ridge. Reconstruction of thrust sheets based on this geometry yielded a minimum displacement of 23 km (Woodward and others, 1991; Connelly and Woodward, 1992).

Truncation of minor stratigraphic units and individual beds along the Snowbird Group-Great Smoky Group contact in the area mapped in this study permits redefinition of the easternmost trace of the Greenbrier fault (Figure 3). These truncations are particularly clear southeast of Cataloochee Divide (Figure 4) where a belt of Longarm Quartzite (approximately 260 m thick) is in contact with different units of the Great Smoky Group, from the middle of the Elkmont Sandstone in the southwest part of the area mapped, to the top of the Thunderhead Sandstone in the northeast. Truncations are less prominent farther southeast in the hanging wall

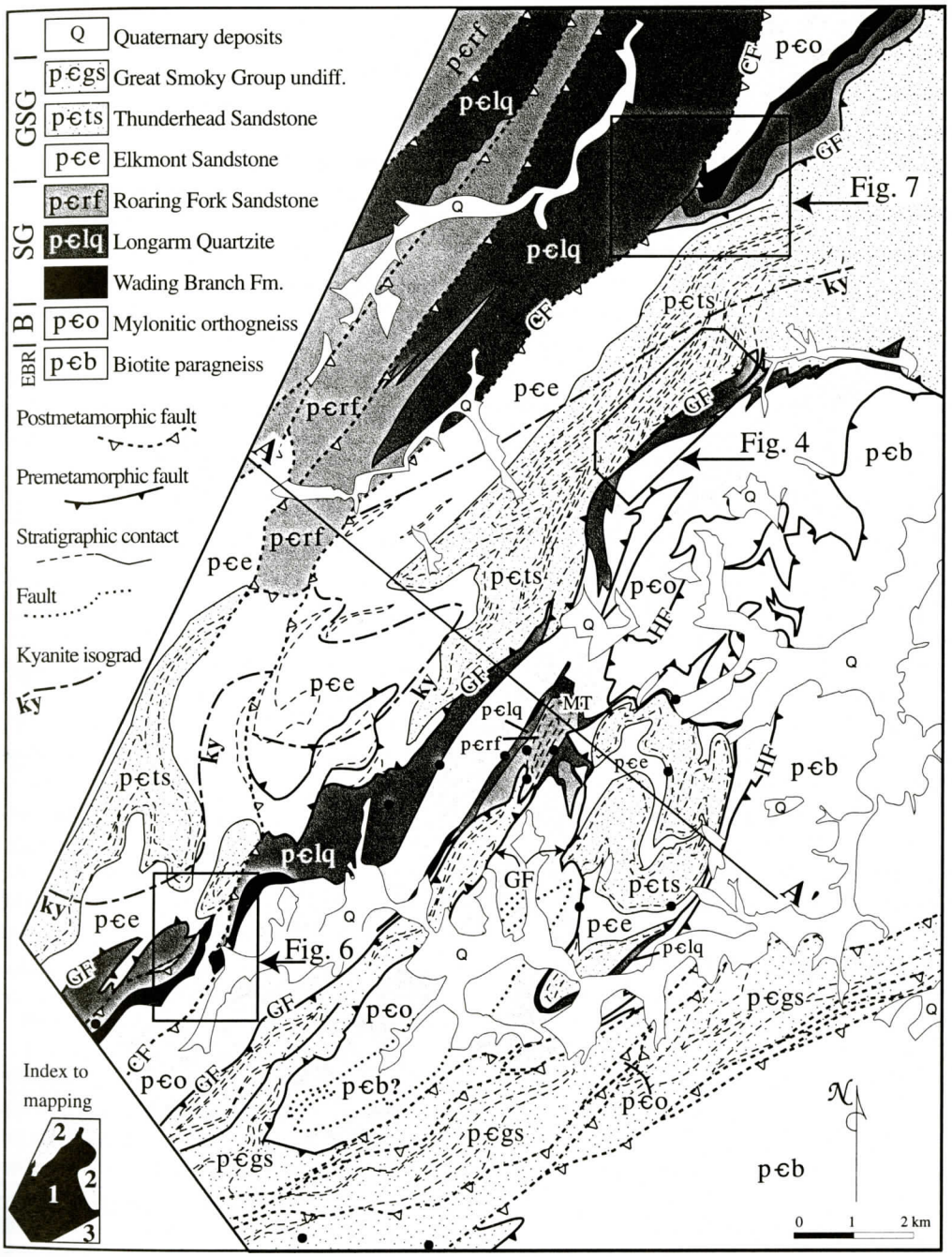

Figure 3. Simplified geologic map of the area studied. Black dots represent location of sandstone samples for point counting. B: basement; CF: Caldwell Fork fault; EBR: eastern Blue Ridge rocks; GF: Greenbrier fault; GSG: Great Smoky Group; HF: Hayesville fault; MT: Moody Top; SG: Snowbird Group. Index to mapping: 1: Montes (1997); 2: Hadley and Goldsmith (1963); 3: Edelman (1983), unpublished 1:24,000 scale map of the Hazelwood quadrangle, N.C.

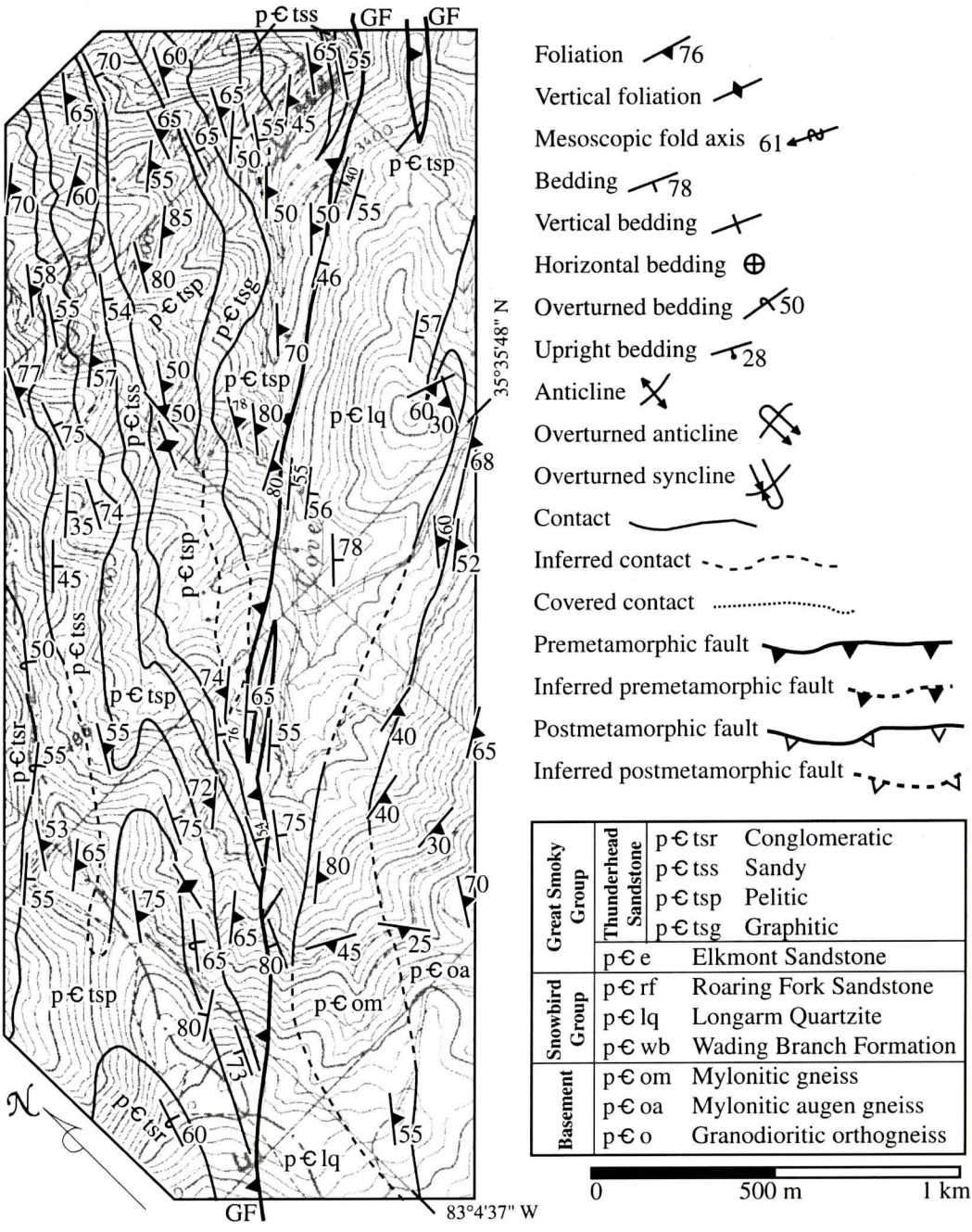

Figure 4. Detailed geologic map of part of the Dellwood quadrangle, NC, showing truncation of sandstone beds in the Thunderhead Sandstone against the Longarm Quartzite as evidence of a faulted contact between the Snowbird Group and the Great Smoky Group.

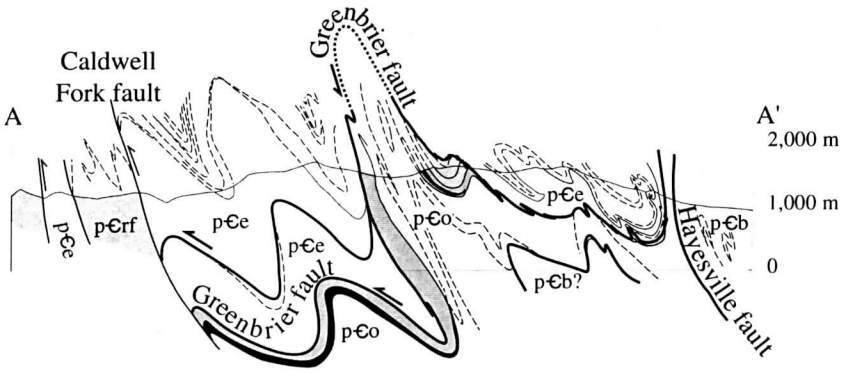

Figure 5. Cross section illustrating truncation of Snowbird Group units in the footwall of Greenbrier fault. All symbols defined in Figure 4.

(Figures 3 and 5), where bedding in units of the Great Smoky Group is nearly parallel to the Greenbrier fault. In the same region, both the unconformable base and transitional top of a 100 m thick section of Longarm Quartzite are exposed along with the lower part of the Roaring Fork Sandstone in the footwall of Greenbrier fault. Farther to the east, however, the Roaring Fork Sandstone and the top of the Longarm Quartzite are truncated against the Greenbrier fault, and the Longarm Quartzite eventually thins to only 20 to 50 m beneath the Greenbrier fault. Therefore, detailed mapping reveals truncations in units above and below the Snowbird Group-Great Smoky Group contact that clearly indicate this contact is a fault.

Caldwell Fork Fault

Postmetamorphic, high angle faults trending NE and NNE have been mapped in this part of the western Blue Ridge. Faults belonging to this set are exposed in the Ravensford anticline (Figure 1), and immediately west of the Cataloochee Divide (Figure 3). We also mapped a set of NE-trending, high angle, postmetamorphic faults along the southeastern corner of the area mapped (Figure 3) that contain retrograde deformation fabrics. These faults have small offsets because metamorphic isograds, and easily traceable contacts such as the Ocoee Supergroup-orthogneiss are not significantly telescoped by these faults, although they are displaced (North Carolina Geological Survey, 1985). The Caldwell Fork fault (here defined) belongs to this set of NNE-trending, postmetamorphic faults (Figures 6 and 7). The Caldwell Fork in the Great Smoky Mountains National Park follows most of the trace of the Caldwell Fork fault northwest of the Cataloochee Divide, and it is better exposed along the Wycle Fork (Figure 6), and along the road to Cataloochee (Figure 7).

The Caldwell Fork fault was originally interpreted as the trace of Greenbrier fault by Hadley and Goldsmith (1963) because it helped explain the stratigraphic thickness contrasts in the Cataloochee Divide region. This fault, however, offsets mesoscopic fabric elements in the area mapped (foliation, mylonitic foliation), as well as the kyanite isograd, and older faults (the Greenbrier fault). Therefore, it is a postmetamorphic structure and should not be correlated with the Greenbrier fault unless the Caldwell Fork fault reactivates a segment of the Greenbrier fault. Reactivation of an earlier fault is unlikely because our mapping shows that the Greenbrier fault here follows the Snowbird Group-Great Smoky Group contact instead (Figure 6). Because the Caldwell Fork fault separates markedly different thicknesses of the Longarm Quartzite, two possibilities must be considered: either it is a postmetamorphic fault with large net slip that juxtaposes sequences originally separated by about 24 km (assuming a 3.5 degrees stratigraphic tapering angle, or

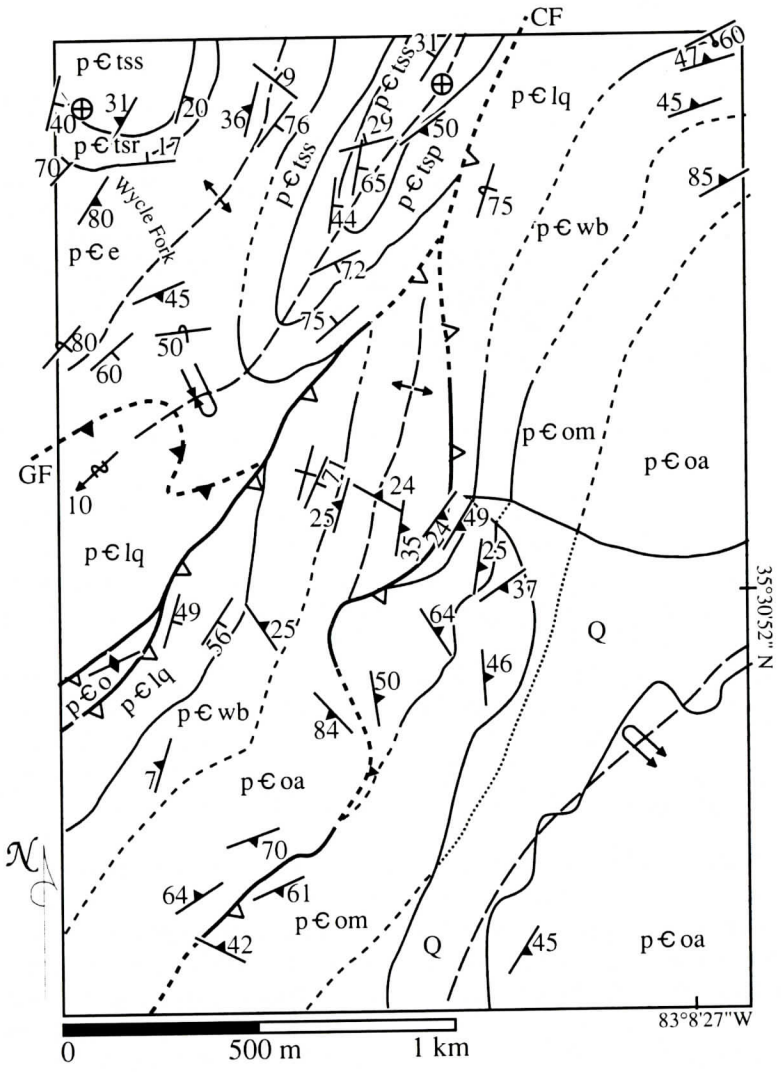

Figure 6. Detailed geologic map of part of the Bunches Bald quadrangle, NC, illustrating the small displacement of the postmetamorphic Caldwell Fork fault that can be inferred from the small offset of identical Wading Branch formation rocks.

about 58 km assuming 1.5 degrees), or it is a minor postmetamorphic fault that reactivated an old growth fault.

The first alternative can be dismissed using independent lines of evidence. First, the Caldwell Fork fault offsets the kyanite isograd by only 1 km (Figure 3). Clearly, a postmetamorphic fault with slip close to 24 km would not only offset isograds an equal amount, but would also juxtapose rocks of greatly different metamorphic grade. Second, the Caldwell Fork fault offsets identical Wading Branch Formation rocks by about 1 km (Figure 6). Because of the characteristically discontinuous nature of the rocks in the Wading Branch Formation, net slip along this fault must be small. A fault with large slip would juxtapose different lithologic types of the Wading Branch Formation. Third, although mappers in this part of the western Blue Ridge (King and others, 1968; North Carolina Geological Survey, 1985) have identified NE-trending postmetamorphic faults in this area,

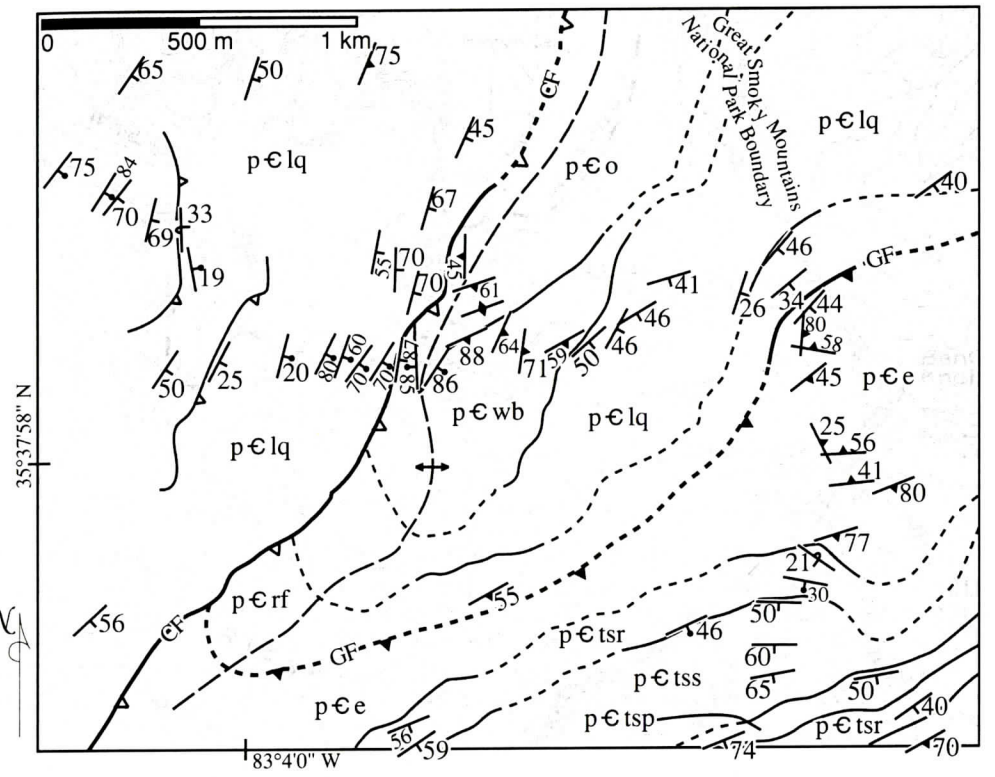

Figure 7. Detailed geologic map of part of the Cove Creek Gap quadrangle, NC, showing contrasting Longarm Quartzite sequences juxtaposed by the postmetamorphic Caldwell Fork fault.

offsets on these faults are characteristically minor.

On the other hand, the postmetamorphic Caldwell Fork fault may have reactivated favorably oriented segments of older structures. Because slip along the postmetamorphic fault is not large enough to explain the thickness changes observed in the Longarm Quartzite, we suggest that the postmetamorphic Caldwell Fork fault reactivated and inverted a favorably oriented segment of a Late Proterozoic normal growth fault that was active during the accumulation of the Longarm Quartzite. The greater thickness of the Longarm Quartzite to the northwest indicates that this was the downthrown block of this northeast-trending normal fault (Figure 8). Whether this fault continued to be active during the accumulation of the Roaring Fork Sandstone, or other younger units, cannot be assessed because these units were removed by the Greenbrier fault.

DISCUSSION

Previous work in this area of the Blue Ridge suggested that the Snowbird Group-Great Smoky Group contact was conformable in the hanging wall of Greenbrier fault, and that elsewhere the Greenbrier fault followed that contact. Early mappers did not separate units within the Great Smoky Group; therefore, truncations above this contact could not be resolved, and truncations below it were explained as being stratigraphic. New mapping in western North Carolina (Figure 3) demonstrates that the Snowbird Group-Great Smoky Group contact is a fault. The Greenbrier fault was originally defined as the fault separating the Snowbird Group from the Great Smoky Group; therefore, the fault we mapped separating these two units in western North Carolina must be the easternmost extension of the Greenbrier fault. This invalidates assumptions regarding the location of

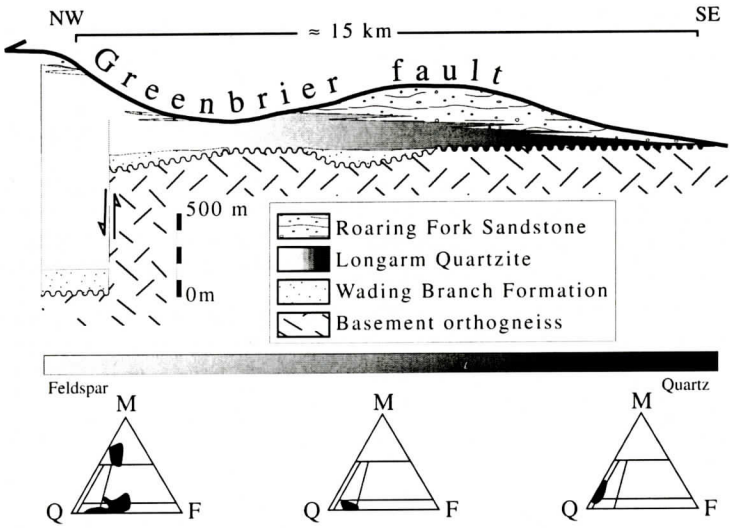

Figure 8. Reconstruction of the stratigraphic relationships among the Snowbird Group units based on bed lengths and relationships shown in figures 2, 3, and 5. The Longarm Quartzite distal downlap relationship to the basement and the Wading Branch Formation is suggested by the sharp contact between the Longarm Quartzite and the Wading Branch Formation, and by changes in Longarm Quartzite sandstone composition. The Caldwell Fork fault reactivates the vertical fault in the left part of the diagram. Relative variation of sandstone composition in the Longarm Quartzite is shown by Q-F-M diagrams.

a large hanging wall ramp where the Greenbrier fault ramps from basement into the Ocoee Supergroup (King and others, 1958; Hadley and Goldsmith, 1963; Woodward and others, 1991; Connelly and Woodward, 1992). This map also indicates that major stratigraphic changes described in previous sections (Figure 2) lie entirely within the footwall of the Greenbrier fault. We explain these changes by a normal fault active during accumulation of the Longarm Quartzite (Figure 8).

The observations presented in this paper support previous paleogeographic models that interpreted the Ocoee basin as a graben separated from the main rifting axis to the east. The Ocoee basin was envisioned having a basement high to the southeast that shed unweathered feldspar into the basin (Hadley, 1970; DeWindt, 1975; Rast and Kohles, 1986). This hypothesis was based on: 1) the dominance of coarse, arkosic sandstone to the south; 2) the thinning of the Longarm Quartzite to the southeast; and 3) paleocurrent indicators that record a southeast to northwest flow direction in the Longarm Quartzite. Rankin (1975) pointed out that the Ocoee Supergroup was deposited west of the main rift axis, on the cratonic side, and was separated from it by a basement horst. This basement high, called the "Unaka horst" by Rast and Kohles (1986), developed early in the history of the basin because the basal unit (Longarm Quartzite) records syntectonic sedimentation. This basement high would be restricted on its eastern side by the normal fault presented herein. It seems unlikely, however, that this basement high provided unweathered feldspar to the Ocoee basin (Hadley and Goldsmith, 1963; Hadley, 1970; DeWindt, 1975) because northwest of the Cataloochee Divide the Longarm Quartzite is arkosic, whereas southeast of it the overall composition of the Longarm Quartzite is truly orthoquartzitic (Figure 2). If an onlap to the southeast existed (King and others 1958), the southeasternmost exposures of Longarm Quartzite should be coarse grained, arkosic, and in general have an immature texture. In contrast, a basement regolith (Wading Branch Formation) is overlain in sharp stratigraphic

contact by thin, orthoquartzitic sandstone of the Longarm Quartzite. We suggest that mature sandstone of the Longarm Quartzite buried the altered basement and its regolith. Thus, the relationship of the Longarm Quartzite to the basement below would be a distal downlap (Figure 8). The provenance of these sands is uncertain, and more comprehensive study of sediment provenance in these sands is necessary to identify source areas. Even though previous studies have presented paleocurrent data (Hadley and Goldsmith, 1963; DeWindt, 1975), the data have been considered unreliable (Rast and Kohles, 1986) because the methodology to subtract complex deformation was not stated.

In summary, redefinition of the trace of the Greenbrier fault in the western Blue Ridge places the entire Snowbird Group in the footwall of this fault. This supports the possibility that the Great Smoky Group may be an eastern correlative of the Snowbird Group telescoped an unknown distance northwestward along the Greenbrier fault. Displacement along this fault, previously delimited to a minimum of 24 km, needs to be reevaluated in light of the new data. A fundamental Late Proterozoic rift fault has been recognized in the easternmost western Blue Ridge. This northeast-trending, northwest-dipping normal fault acted as the eastern border of the Ocoee basin, and probably hindered east-west sediment dispersal.

ACKNOWLEDGMENTS

Funded by the Geological Society of America Research Grant 5664-95, the University of Tennessee Science Alliance Center of Excellence, the Tectonics and Structural Geology Research Facility, a Swingle Fellowship from the Department of Geological Sciences of the University of Tennessee, and COLCIENCIAS. Critical reviews by William Dunne, Steve Kish, Peter Lemiszki, and Kevin Stewart improved the manuscript. We remain culpable, however, for all errors of fact and interpretation.

REFERENCES CITED

Abbott R. N., and Raymond, L. A., 1984, The Ashe metamorphic suite, northwest North Carolina: metamorphism and observations on geologic history: American Journal of Science, v. 284, p. 350-375.

Adams, M. G., and Su, Q., 1996, The nature and timing of deformation in the Beech Mountain thrust sheet between the Grandfather Mountain and Mountain City windows in the Blue Ridge of northwestern North Carolina: The Journal of Geology, v. 104, p. 197-213.

Butler, J. R., 1973, Paleozoic deformation and metamorphism in part of the Blue Ridge thrust sheet, North Carolina: American Journal of Science, v. 273-A, p. 72-88.

Carpenter, R. H., 1970, Metamorphic history of the Blue Ridge province of Tennessee and North Carolina: Geological Society of America Bulletin, v. 81, p. 749-762.

Carter, M. W., Hatcher R. D. Jr., Geddes D. J., Martin S. L., and Montes C., 1995a, New lithotectonic framework in the western Blue Ridge, Southern Appalachians; building on earlier USGS work: Geological Society of America Abstracts with Programs, v. 27, p. 223.

Carter, M. W., Geddes, D. J., Hatcher, R. D., Jr., and Martin, S. L., 1995b, Stratigraphic and structural relationships in the western Blue Ridge foothills of southeastern Tennessee, *in* Driese, S. G., ed., Guidebook for field trip excursions, Southeastern Section Geological Society of America: Knoxville, University of Tennessee, Department of Geological Sciences Studies in Geology, v. 24, p. 91-128.

Connelly, J. B., and Dallmeyer, R. D., 1993, Polymetamorphic evolution of the western Blue Ridge: Evidence from $^{40}Ar/^{39}Ar$ whole-rock slate/phyllite and muscovite ages: American Journal of Science, v. 293, p. 322-359.

Connelly, J. B., and Woodward, N. B., 1992, Taconian foreland-style thrust system in the Great Smoky Mountains, Tennessee: Geology, v. 20, p. 177-180.

Costello, J. O., and Hatcher, R. D., Jr., 1991, Problems of stratigraphic correlation between Great Smoky, Snowbird, and Walden Creek Groups between the Great Smoky National Park, central east Tennessee, and Ocoee Gorge, southeastern Tennessee, *in* Kish, S.A., ed., Studies of Precambrian and Paleozoic stratigraphy in the western Blue Ridge: Carolina Geological Society Guidebook, p. 13-25.

Dallmeyer, R. D., 1975, Incremental $^{40}Ar/^{39}Ar$ ages of biotite and hornblende from retrograded basement gneisses of the southern Blue Ridge: Their bearing on the age of Paleozoic metamorphism: American Journal of Science, v. 275, p. 444-460.

DeWindt, J. T., 1975, Geology of the Great Smoky Mountains, Tennessee and North Carolina, with road log for field excursion, Knoxville-Clingman's Dome-Maryville: Compass, v. 52, p. 73-129.

Fullagar P. D., Goldberg, S. A., and Butler, R. J., 1997, Nd and Sr isotopic characterization of crystalline rocks from the southern Appalachian Piedmont and Blue Ridge, North and South Carolina, *in* Sinha, A, K., Whalen, J. B., and Hogan, J. P., eds., The nature of magmatism in the Appalachian orogen: Boulder, Colorado, Geological Society of America Memoir 191, p. 161-

179.

Goldberg, S. A., Butler, R., and Fullagar, P. D., 1986, The Bakersville dike swarm: Geochronology and petrogenesis of Late Proterozoic basaltic magmatism in the southern Appalachian Blue Ridge: American Journal of Science, v. 286, p. 403-430.

Hadley, J. B., 1970, The Ocoee Series and its possible correlatives, *in* Fisher, G. W., Pettijohn, F. J., Reed, J. C., and Weaver, K. N., eds., Studies of Appalachian geology: Central and southern: New York, Interscience Publishers, p. 247-259.

Hadley, J. B., and Goldsmith, R., 1963, Geology of the eastern Great Smoky Mountains, North Carolina and Tennessee: U.S. Geological Survey Professional Paper 349-B, 118 p.

Hardeman, W. D., 1966, Geologic map of Tennessee: Tennessee Division of Geology, scale 1:250,000.

Hatcher, R. D., Jr., 1989, Tectonic synthesis of the U.S. Appalachians, *in* Hatcher, R. D., Jr., Thomas, W. A., and Viele, G. W., eds., The Appalachian-Ouachita orogen in the United States: Boulder, Colorado, Geological Society of America, The Geology of North America, v. F-2, p. 511-535.

Hatcher, R. D., Jr., Thomas, W. A., Geiser, P. A., Snoke, A. W., Mosher, S., and Wiltschko, D. V., 1989, Alleghanian orogen, *in* Hatcher, R. D., Jr., Thomas, W. A., and Viele, G. W., eds., The Appalachian-Ouachita orogen in the United States: Boulder, Colorado, Geological Society of America, The Geology of North America, v. F-2, p. 233-318.

Hoffman, P. F., 1991, Did the breakout of Laurentia turn Gondwanaland inside-out?: Science, v. 252, p. 1409-1412.

Keller, F. B., 1980, Late Precambrian stratigraphy, depositional history, and structural chronology of part of the Tennessee Blue Ridge [unpublished Ph. D. thesis]: New Haven, Connecticut, Yale University, 351 p.

King, P. B., Neuman, R. B., and Hadley, J. B., 1968, Geology of the Great Smoky Mountains National Park, Tennessee and North Carolina: Geological Survey Professional Paper 587, 23 p.

King, P. B., Hadley, J. B., Neuman, R. B., and Hamilton, W., 1958, Stratigraphy of Ocoee Series, Great Smoky Mountains, Tennessee and North Carolina: Geological Society of America Bulletin, v. 69, p. 947-966.

Miller, C. F., Hatcher, R. D., Jr., Harrison, T. M., Coath, C., and Gorish, E. B., 1998, Cryptic crustal events elucidated through zone imaging and ion microprobe studies of zircon, southern Appalachian Blue Ridge, North Carolina-Georgia: Geology, v. 26, p. 419-422.

Milton, D. J., 1983, Garnet-biotite geothermometry confirms the premetamorphic age of the Greenbrier fault, Great Smoky Mountains, North Carolina: Geological Society of America Abstracts with Programs, v. 15, p. 90.

Montes, C., 1997, The Greenbrier and Hayesville faults in central-western North Carolina [unpublished M.S. thesis]: Knoxville, University of Tennessee, 145 p.

North Carolina Geological Survey, 1985, Geologic map of North Carolina: North Carolina Geological Survey, scale 1:500,000.

Odom, A. L., and Fullagar, P. D., 1984, Rb-Sr whole-rock and inherited zircon ages of the plutonic suite of the Crossnore Complex, southern Appalachians, and their implications regarding the time of opening of the Iapetus Ocean, *in* Bartholomew, M. J., ed., The Grenville event in the Appalachians and related topics: Geological Society of America Special Paper 194, p. 255-262.

Quinn, M. J., 1991, Two lithotectonic boundaries in western North Carolina: Geologic interpretation of a region surrounding Sylva, Jackson County [unpublished M.S. thesis]: Knoxville, University of Tennessee, 223 p.

Quinn, M. J., and Wright, J. E., 1993, Extension of Middle Proterozoic (Grenville) basement into the eastern Blue Ridge of southwestern North Carolina: Results from U-Pb geochronology: Geological Society of America Abstracts with Programs, v. 25, p. A483.

Rankin, D. W., 1975, The continental margin of eastern North America in the southern Appalachians: The opening and closing of the Proto-Atlantic Ocean: American Journal of Science, v. 275-A, p. 298-336.

Rast, N., and Kohles, K. M., 1986, The origin of the Ocoee Supergroup: American Journal of Science, v. 286, p. 593-616.

Rodgers, J., 1972, Latest Precambrian (Post-Grenville) rocks of the Appalachian region: American Journal of Science, v. 272, p. 507-520.

Schwab, F. L., 1976, Depositional environments, provenance, and tectonic framework: Upper part of the late Precambrian Mount Rogers Formation, Blue Ridge province, southwestern Virginia: Journal of Sedimentary Petrology, v. 46, p. 3-13.

Su, Q., Goldberg, S. A., and Fullagar, P. D., 1994, Precise U-Pb zircon ages of Neoproterozoic plutons in the southern Appalachian Blue Ridge and their implications for the initial rifting of Laurentia: Precambrian Research, v. 68, p. 81-95.

Thomas, W. A., 1991, The Appalachian-Ouachita rifted margin of southeastern North America: Geological Society of America Bulletin, v. 103, p. 415-431.

Wehr, F., and Glover, L., III, 1985, Stratigraphy and tectonics of the Virginia-North Carolina Blue Ridge: Evolution of a late Proterozoic-early Paleozoic hinge zone: Geological Society of America Bulletin, v. 96, p. 285-295.

Woodward, N. B., Connelly, J. B., Walters, R. R., and Lewis, J. C., 1991, Tectonic evolution of the Great Smoky Mountains: Studies of Precambrian and Paleozoic stratigraphy in the western Blue Ridge, *in*, Kish, S. A., ed. Carolina Geological Society field trip guide, p. 57-68.

SOUTHEASTERN GEOLOGY
V. 39, No. 1, November 1999, p. 51-60

WATER SOURCES OF WAKULLA SPRINGS, WAKULLA COUNTY, FLORIDA: PHYSICAL AND URANIUM ISOTOPIC EVIDENCES

HONGSHENG CAO, JAMES B. COWART, AND JOHN K. OSMOND

Department of Geology
Florida State University
Tallahassee, FL 32306, U.S.A.

ABSTRACT

Wakulla Springs is one of the largest and deepest freshwater springs in the world. The hydrologic system in the Wakulla Springs area is extremely vulnerable to pollution because of the highly permeable limestones that comprise the aquifer and its unconfined exposure to direct recharge. The main tunnel of the Wakulla Springs splits into four major tunnels (tunnel A, B, C, and D), which are in a branch-work configuration.

In recent years, environmentalists and residents have been concerned about development around the Wakulla Springs area. The contaminated storm water runoff, sewage disposal, and sanitary landfills from the Tallahassee urban area have a potential to pollute the natural water sources of the Wakulla Springs. Potential pollution sources include the disposal of chemicals, the leaks from underground storage tanks, the discharges from sewage treatment plants and septic tanks, fertilizers, herbicides, and pesticides. The sources of the water that feeds the spring are uncertain. Therefore, the threats of water pollution in the Wakulla Springs area make the evaluation of its water sources necessary.

Uranium isotopes in water have been shown to be useful as tracers to identify mixing water sources. The identities of different water sources can be discriminated by their uranium concentrations and uranium isotopic ratios ($^{234}U/^{238}U$). Uranium results indicate that the Wakulla Springs' pool water is a mixture of the tunnels' waters and local ground and surface waters. Tunnel A and Tunnel C are fed by ground water underlying Woodville, whereas Tunnel B and Tunnel D may be fed by the ground waters that underlie Tallahassee and its north.

INTRODUCTION

Wakulla Springs, one of the largest and deepest freshwater springs in the world and an attractive state park, is located in Wakulla County within the Woodville Karst Plain, Florida (Figure 1). Wakulla Springs forms the headwaters of the Wakulla River, which flows south to the Gulf of Mexico. It has an average discharge rate of 99.3 m^3/s (ranging from 6.4 m^3/s to 486 m^3/s). The basin of the spring covers approximately 1.21×10^4 m^2. The water temperature remains a relatively constant 21.1°C year-round. The spring issues from the Floridan aquifer system. The highly porous nature of the Floridan aquifer makes it an abundant source of fresh water for the area. All the public water supply in the area is drawn from wells that penetrate the Floridan aquifer. Regional groundwater flow is from north to south at approximately 3 m/day (Hendry and Sproul, 1966).

The hydrologic system in the Wakulla Springs area is extremely vulnerable because of the highly permeable limestones that comprise the aquifer and its unconfined exposure to direct recharge. In recent years, environmentalists and residents have been concerned about development around the Wakulla Springs area. The contaminated storm water runoff, sewage disposal, and sanitary landfills from the Tallahassee urban area have a potential to pollute the natural water sources of the Wakulla Springs. Potential pollution sources include the disposal of chemicals, the leaks from underground storage tanks, the discharges from sewage treatment plants and septic tanks, fertilizers, herbicides, and pesticides. The sources of the water that feeds the spring are uncertain. Therefore, the threats of water pollution in Wakulla Springs and the Woodville Karst Plain make the

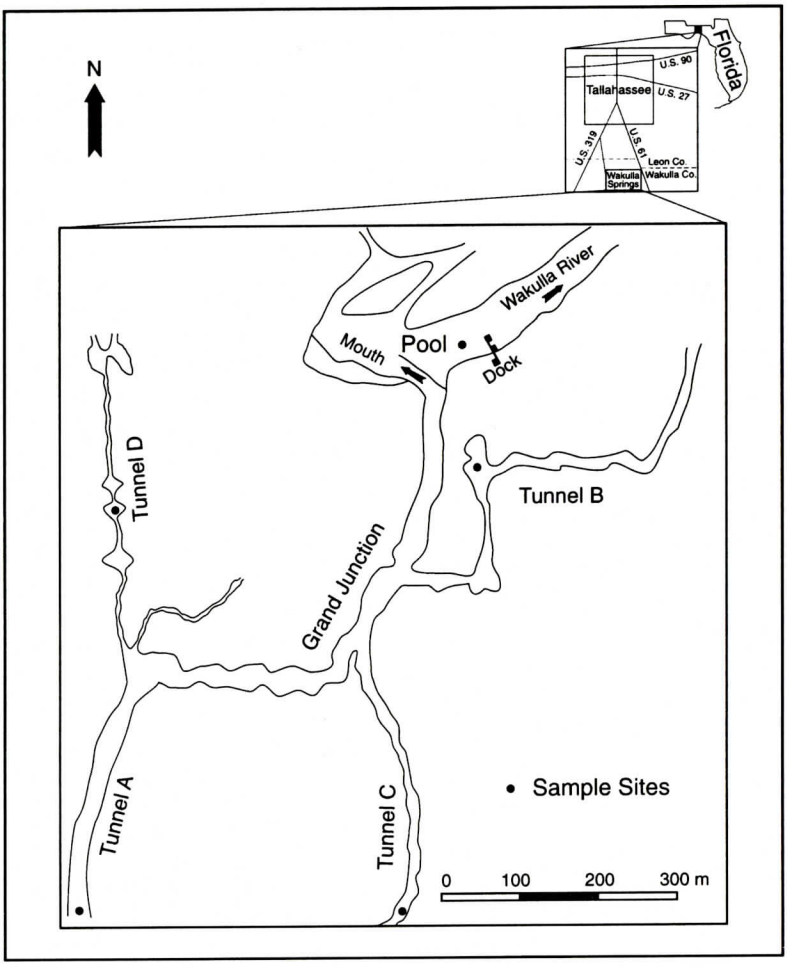

Figure 1. Location of the Wakulla Springs and sample sites, Wakulla County, Florida.

evaluation of the water sources necessary.

In the Tallahassee area the aquifer is overlain by the sand and red clay of the Miccosukee Formation which act as a confining layer. To the south of Tallahassee, in the Woodville Karst Plain, the Miccosukee Formation is absent and the limestones of the Floridan aquifer are either exposed at the surface or overlain by a few meters of coarse Pleistocene sand. Most of the rain that falls on the city of Tallahassee eventually infiltrates through the soil, recharging the shallow surficial aquifer, or finds its way on the surface into lakes and possibly into the exposed Floridan aquifer in the Woodville Karst Plain.

There are three naturally occurring uranium isotopes: ^{238}U, ^{235}U, and ^{234}U. The ^{238}U accounts for the majority of the natural uranium abundance (99.2743%), and is the parent of the ^{238}U decay chain (Faure, 1986). The ^{235}U (0.7200%) isotope is the parent of the actinium series, an independent decay chain, which is not going to be discussed in this study. The ^{234}U isotope is the third generation daughter of ^{238}U and accounts for 0.0057% of all naturally occurring uranium.

In a closed system, ^{234}U and ^{238}U will be in equilibrium ($^{234}U/^{238}U = 1$). However, in open systems, such as weathering, dissolution and water circulation, the activity ratios of these two isotopes can vary and are not 1:1 (unity). Many samples of freshwater show enrichments of ^{234}U rather than deficiencies. Generally, sur-

face waters have lower concentrations and higher activity ratios (displaying an excess of daughter ^{234}U).

The mechanism of the fractionation of ^{234}U with respect to its radiogenic parent ^{238}U in natural waters has been discussed in connection with the physiochemical nature of alpha recoil atoms in the silicate lattice. Fractionation between ^{238}U and ^{234}U occurs in secondary minerals and in groundwater (Cherdytsev, 1971). Fractionation puts a fingerprint on the water in terms of an isotopic activity ratio ($^{234}U/^{238}U$) so that the hydrologic patterns of the area can be resolved (Osmond and others, 1968). This state (activity ratio not equal to 1) is known as isotopic disequilibrium, which can occur for several different reasons. Kigoshi (1971) first explained the mechanisms of the uranium fractionation based on his experiment. Possible mechanisms for fractionation have been categorized and described in details (Osmond and Cowart, 1976).

The uranium isotopic disequilibrium method has been extensively applied to delineate many hydrologic regimes in various sandstone and carbonate aquifer systems world wide (Osmond and others, 1968; Kaufman and others, 1969; Osmond and Cowart, 1976; Cowart, 1977, 1980; Bonotto and Andrews, 1993; Kronfeld and others, 1991, 1994; Lienert, 1994; Hussain, 1995; Zielinski and others, 1997). Dissolved uranium isotopes in water have been shown to be useful as tracers to identify mixing sources. The identities of differing water sources can be discriminated by their uranium (^{238}U) concentrations and their uranium isotopic ratios ($^{234}U/^{238}U$).

The objectives of this study are: 1) to examine the uranium isotopic signatures of the Wakulla Springs; 2) to determine probable sources of the water flowing out of Wakulla Springs based on the uranium fingerprints; 3) to determine if uranium isotopes can help trace regional groundwater movement; 4) to evaluate the interaction pattern between groundwater and surface water in the Wakulla Springs area.

GEOLOGICAL SETTING

In the Wakulla Springs vicinity, the Floridan aquifer system is composed of three Tertiary limestone units (in descending order): the St. Marks Formation, the Suwannee Limestone, and the Ocala Group. The St. Marks Formation is the uppermost carbonate unit in the Woodville Karst Plain. It is a "white to pale orange fossiliferous calcilutitic limestone" (Rupert and Spencer, 1988). It contains intermittent thin beds of clay and abundant mollusk and foraminiferal molds. The Suwannee Limestone is a white to pale orange calcarenitic to biocalcarenitic limestone and orange calcilutite. The Suwannee Limestone contains intermittent beds of light brown dolomite. The Ocala Group is a light tan limestone and a brown dolomite.

The aquifer in the study area is semi-confined and contains artesian springs. Recharge is from runoff both through a diffuse system of porous sands and directly into the tunnel system via sinkholes. The tunnel system feeding Wakulla Springs is developed in the Suwannee Limestone unit (Rupert and Spencer, 1988). Unconformably overlying the limestone units is approximately 2.7 m of undifferentiated sand and clay of Pleistocene to Recent in age. These sediments are alluvial and aeolian deposits predominantly composed of quartz sands. These porous sands allow local recharge into the aquifer system. The topography surrounding the Wakulla Springs slopes gently southward with an elevation of approximately 10.6 m above mean sea level. The surface gradient is approximately 75.77 centimeters per kilometer with a southeastwardly directed potentiometric surface (Rupert and Spencer, 1988).

At a distance of about 274.32 m into the main tunnel, in a room named the Grand Junction, the main tunnel splits into four major separate tunnels (Stone, 1988), which are identified as A, B, C, and D (Figure 1). The tunnels, which feed the Wakulla Springs, are in a branch-work configuration.

Tunnels A and C head to the south, while tunnel B trends northeastward and tunnel D heads north. The tunnels vary in size, but are large on average. The dimensions of the tunnels

average 14.33 m high and 35.66 m wide. Tunnel B was explored to a total distance of 1371.6 m in length from the spring mouth (the maximum extent explored). The deepest depth recorded is 109.72 m below the spring pool surface in tunnel B near the 1371.6 m limit. Water flow in all tunnels is towards the Grand Junction, and ultimately northward to the spring mouth. Interestingly, this flow is generally in opposition to the local hydrologic gradient. Tunnels B, C, and D carry clear water, whereas tunnel A carried tannic water (Clemens, 1988). Tunnel A contributes significantly in terms of volume and represents a shallow source (an inference based on its tannic water). Tunnel A always carries some component of tannic water. Periodically, it becomes extremely tannic following periods of precipitation. Input from the tannic tunnel frequently determines the spring's overall clarity on a daily basis. These tunnels are just a portion of an extensive network of interconnected and possibly joint controlled tunnels underlying the Woodville Karst Plain. Each of these tunnels is believed to carry different source waters.

METHODS

In order to accomplish the goals of this study, three groups of samples were collected: 1) Wakulla Springs pool samples (labeled pool), 2) Wakulla Springs tunnel samples (labeled tunnel), and 3) regional water samples. Those samples collected at the surface of the main pool, which forms the headwaters of the Wakulla River, are referred to as 'pool samples' while those samples, collected within four subterranean tunnels of the Wakulla Springs, are referred to as 'tunnel samples'. Regional samples were collected from Tallahassee city wells (labeled tcw), local deep wells (labeled wvw), and local creeks (Table 1 and Table 2). The pool and tunnel samples were all collected using the cave diving sampling method with the help of cave divers. Sampling depth ranged from 3 m to 30 m below spring surface for the pool samples.

Generally, about 14.0 liters water samples are enough for this purpose. Sample containers are subjected to diluted clean nitric acid (HNO_3) and hydrochloric acid (HCl) treatments first in the laboratory. The containers are rinsed three times by the sampling water before water samples are collected. Though water samples from wells and tunnels are generally clear and without visible particulate matter, they are all filtered through 0.45 μm filter to remove any organic matter or fine sediments that may interfere in the processing.

Pretreatment, co-precipitation, ether extraction, anion exchange, and electroplating are the major steps for uranium separation before the measurement by alpha spectrometry. Pretreatment involves the addition of 2 ml of ^{232}U tracer spike, 5 ml of dilute clean iron nitrate ($Fe[NO_3]_3$) solution, and 20 ml of 8N clean nitric acid in each bottle of the sample (3.5 liter). The next step involves the co-precipitation of uranium and iron after heating the bottles to 100 °C and adding ~ 20 ml of ammonia hydroxide (NH_4OH). The iron flocculates form at this stage. Ferric hydroxide scavenges many elements including the uranium and eventually settles on the bottom of the bottle. The separated and dried flocculate is dissolved in 8N clean hydrochloric acid (HCl) and evaporated to dryness. The dried sample is completely dissolved in approximately 30 ml of clean 8N hydrochloric acid (HCl). Approximately 30 ml of pure ether is used for ether extraction. The sample and acid phase is allowed to drain back into the 250 ml beaker, and the ether and iron phase is discarded. After ether extraction, the sample is allowed to evaporate to dryness before the anion exchange process is conducted. The purpose of the anion exchange columns is to separate other elements from uranium. The anion exchange procedure involves two column runs: separating uranium from other elements and purifying uranium. The basic steps are similar in each of these two column runs: a) cleaning columns; b) conditioning columns; c) loading sample; d) washing columns; and e) collecting uranium. In the first column, a prepared ion exchange column is washed with 40 ml 0.1N clean hydrochloric acid (HCl). Then the columns are conditioned by adding 30 ml 8N clean hydrochloric acid (HCl) before loading samples in 8N hydrochloric acid (HCl). Elute columns with 30 ml 0.1N clean hydro-

Table 1. Uranium isotopic data for the pool and tunnel water samples of the Wakulla Springs.

Samples	$^{234}U/^{238}U$ (a)	U (ppb) (b)	1/U
Tunnel A	0.81	0.64	1.6
Tunnel B	0.91	0.58	1.7
Tunnel C	0.82	0.62	1.6
Tunnel D	0.88	0.57	1.8
Pool 1	0.84	0.63	1.59
Pool 2	0.81	0.46	2.17
Pool 3	0.79	0.64	1.56
Pool Average	0.813	0.577	1.73

(a) Uncertainty (2σ) ranges from ± 0.02 to ± 0.04.

(b) Uncertainty (2σ) ranges from ± 0.02 to ± 0.04.

chloric acid (HCl) twice to release uranium from the resin and collect the elutant in a labeled Teflon beaker. The uranium in the Teflon beaker is brought to dryness under the heat lamps. The second column run involves the use of 8N HNO_3 instead of 8N HCl for cleaning. The dried residue is dissolved in 10 ml of 8N clean nitric acid (HNO_3) and the ion exchange column is conditioned by 30 ml 8N clean nitric acid (HNO_3). The sample in 10 ml of 8N clean nitric acid (HNO_3) is loaded to the column. Columns are eluted twice with 30 ml 0.1N clean hydrochloric acid (HCl) to release the uranium from the resin and then collect the purified uranium fraction in a Teflon beaker. Evaporate the 60 ml 0.1N hydrochloric acid (HCl) and uranium to dryness. The dried sample is dissolved in 5 ml of 2N clean ammonia chloride (NH_4Cl, pH = 2.52-2.60). The electroplating is conducted with an electroplating assembly set for about an hour and the planchet is flamed for 30 seconds to fix the deposited radionuclides on the planchet. The sample is now ready for alpha spectrometer measurement. The detailed procedures are described by Osmond and Cowart (1976) and Lally (1992).

RESULTS

The samples labeled "Tunnel A, B, C, and D" were collected during a dry season from tunnel A, B, C, and D, respectively. All four samples were clear, with no visible particulate matter. B, C and D tunnels remain clear year round whereas tunnel A often had tannic components. Table 1 contains the uranium data of water samples collected from the pool and four main tunnels of the Wakulla Springs. The average uranium concentration is 0.6025 ppb and the uranium activity ratios range from 0.81 to 0.91 for the four main tunnels while pool samples have an average uranium concentration of 0.577 ppb and an average activity ratio of 0.813.

The karstic deep ground water samples (labeled WVW 1 and WVW 2) demonstrate low activity ratios and high concentrations, whereas non-karstic samples (most of the city wells) and surface water demonstrate high activity ratios and very low concentrations. Table 2 contains the uranium data of regional samples neighboring the Wakulla Springs. This group of samples can be categorized into two types: the groundwater samples from the deep wells in the Woodville Karst Plain and the Tallahassee city wells, and the surface water samples from the creeks in the Woodville Karst Plain. The samples from the two deep wells have a very high uranium concentration and a very low activity ratio whereas the samples from the Tallahassee city wells have a medium concentration and ratio, and the surface samples have a very low concentration and a high ratio. The activity ratios range from 0.488 to 1.47 and the concentrations range from 0.035 ppb to 10.19 ppb for the regional samples. Uranium isotopic fingerprints conducted on water samples taken from this area reveal that tunnels B and D carry regional groundwater, whereas tunnel A and possibly tunnel C have local groundwater and recent surface water components. Relative to the global groundwater uranium data (Osmond and Cowart, 1976), Wakulla Springs has anomalously low $^{234}U/^{238}U$ isotopic ratios and high uranium concentrations.

Table 2. Uranium data for the regional water samples around the Wakulla Springs.

Samples	$^{234}U/^{238}U$ (a)	U (ppb) (b)	1/U
WVW 1	0.488	10.19	0.1
WVW 2	0.557	8.44	0.07
TCW 5	1.01	0.53	1.89
TCW 12	0.88	0.47	2.13
TCW 15	0.97	0.56	1.79
TCW 20	0.91	0.43	2.33
TCW 22	1.06	0.35	2.86
TCW 27	0.88	0.37	2.7
Black Creek	1.47	0.035	28.57
Lost Creek	1.087	0.328	3.05
Fisher Creek	1.8	0.04	25
Jump Creek	1.09	0.143	6.99

(a) Uncertainty (2σ) ranges from ± 0.02 to ± 0.04.

(b) Uncertainty (2σ) ranges from ± 0.02 to ± 0.04.

DISCUSSION

In order to produce mixing diagrams with straight lines, reciprocal uranium concentration is used rather than concentration itself. The isotopic data are graphed using uranium activity ratio ($^{234}U/^{238}U$) versus reciprocal of uranium concentration (1/U). A polygon can be constructed using the Wakulla Springs tunnels as possible sources of the mixture water of the pool water samples. The Wakulla Springs pool samples and their average and the four major tunnel samples are plotted (Figure 2). The polygon indicates the possible plotting region for pool samples if the tunnels are the sole source. All three pool samples were plotted in the tunnels A and C neighborhood. The pool samples do not plot near the center of the tunnel polygon. From the polygon, it can be directly concluded that the four main tunnels have a distinctive water source. This would be the case if the tunnels were the sole source of the pool water sampled. Therefore, the four major tunnels are not the sole source of the pool samples.

There are two principal components for the pool water sources of Wakulla Springs. The main component has a high uranium isotopic activity ratio and low uranium concentration, which represents locally surface water and shallow water. It will become dominant during periods of heavy precipitation. The second component originates regionally and represents deeper leaching water.

The Wakulla Springs' pool samples consist of source waters with a high uranium activity ratio and low uranium concentration mixed with low uranium activity ratio and high uranium concentration. The mixing creates an isotopic fingerprint exhibited in the pool samples. Since the pool water samples and their average fall outside of the polygons, it can be confirmed that the pool water at Wakulla Springs is possibly a mixture of the water from the tunnels and local surface water. However, it is the tunnels that provide the greatest volume of water to the spring and the tunnel A should be the main provider.

Pool sample variations are at least in part non-random; i.e., not simply due to uncertainty variations. The Wakulla Springs pool samples scatter around tunnels A and C of the tunnels' envelope. It is possible that the dilution components come from surface or shallow horizons. The resulting pool water is a mixture of tunnels A and C, surface water, and shallow groundwater. Another possibility is that some of the tunnels do not contribute as much as others. Tunnel A is by far the largest of all caves and contributes tannic flow characteristic of shallow components in wet seasons. In addition, tunnel samples are more concentrated than the regional ground and surface waters and less concentrated than the local groundwater. This may possibly be due to the vigorous leaching or less dilution occurring in the tunnels and local deep groundwater.

The principal recharge area for Wakulla Springs is probably located in the Leon Sinks area of southern Leon County. Major tunnel systems extending from the Leon Sinks area through Wakulla County near Wakulla Springs have been connected by cave divers and is be-

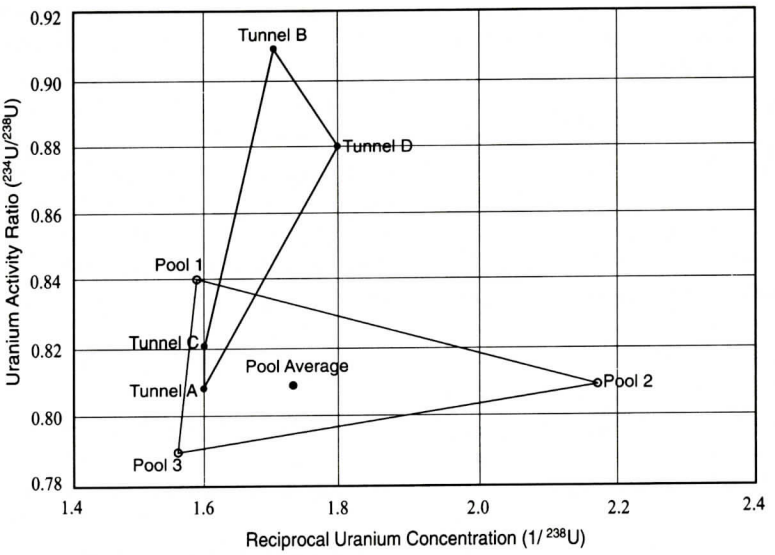

Figure 2. Uranium isotopic polygon of Wakulla Springs' pool and tunnel samples.

lieved to be represented as tunnel A in Wakulla Springs. Indeed, this lineation corresponds to the potentiometric surface. There may also be a recharge component northeast of the Springs. Due to the close proximity of sinkholes to Wakulla Springs and the great volume of water discharging the Wakulla Springs, some tunnels carry more "local" water than others (i.e., tunnels B and C).

To determine whether isotopic variations exhibited in pool samples are a function of rainfall, precipitation records and activity ratios were compared (Macesich, 1991; Whitecross, 1995). Wakulla Springs' pool water activity ratios and concentrations varied with precipitation (Macesich, 1991). It would seem intuitive that heavy rainfall would result in a higher activity ratio. Wakulla Springs is best described as a flushing system overwhelmed by an isotopic signature of locally recharged water during wet periods. Comparison of Wakulla Springs pool samples activity ratios and precipitation data suggests that the activity ratios are low during dry seasons (Whitecross, 1995). Activity ratios are used exclusively as a parameter in correlation since they are the more stable characteristic of the water. Concentration, because of dilution and precipitation effects, is a more haphazard characteristic of the water. Different sources from all depth horizons continually contribute to Wakulla Springs. Tunnel A, for example, carries a low uranium activity ratio and is the largest of all the tunnels contributing to the spring. During wet seasons, there is a greater influx of recharge from many horizons. Flushing of the aquifer on every level occurs. Those local contributors which carry a high uranium activity ratio may heavily contribute and overwhelm the isotopic signature (or sufficiently mix) so that the prevailing uranium activity ratio during wet seasons is high.

In other words, tunnels A and C, which have a relatively lower activity ratio and lower concentration than the two other tunnels, may constantly contribute regardless of the season and overrides the local isotopic signature of the water. This would explain low activity ratios during dry seasons and high activity ratios during wet seasons.

However, the water in the tunnels probably has its own distinctive sources as demonstrated by polygon tunnel water signatures. The uranium data for tunnels B and D are similar to the data of the Tallahassee city wells (Figure 3). Diver observation suggests that tunnel B is a very deep, clear path of flow. This suggests that tunnels B and D are being supplied from the same water source that underlie the city of Tal-

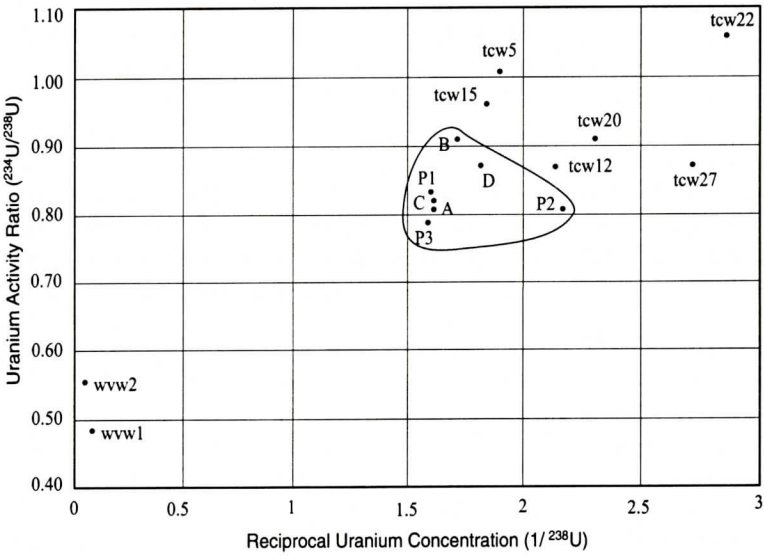

Figure 3. Uranium isotopic variation of Wakulla Springs' samples and regional samples.

lahassee. Therefore, the recharge area for tunnels B and D is located in southern Georgia and northern Leon County, Florida. The uranium fingerprints of tunnels A, B, C, and D are different from those of two karstic deep public supply wells (labeled WVW 1 and WVW 2) northeast of Wakulla Springs (Figure 3). This suggests that tunnels A, B, C, and D don't have the same origin as the two deep wells, located in the Woodville area of the Woodville Karst Plain. Though diver observation also suggests that tunnel C is very deep and clear, tunnels A and C are probably recharged locally due to the unconfined aquifer in this area. These interpretations are constrained by the fact that samples of the tunnels were only obtained during a dry season when the water was clear.

The sources of uranium in this area are phosphorites, clays, and other clastic detritus that are found in abundance in the St. Marks Formation and the undifferentiated sand and clay of Pleistocene to Recent in age. Both the St. Marks Formation and the unconsolidated sands and clays have a relatively high radioactivity compared to purer, deeper formations in the Floridan aquifer system such as the Suwannee Limestone and the Ocala Group limestone. Ground waters of the Woodville Karst Plain exhibit a uranium isotopic fingerprint, which appears to be inconsistent with the models of fractionation. Reducing waters normally produce waters with low concentrations and high activity ratios due to the insolubility of uranium in reducing environments. However, here the activity ratios are often very low, well below equilibrium value. It is as if the ^{238}U is being preferentially mobilized. This is not presumed to be the case. The low activity ratios are probably caused by dissolution of uranium from grain surfaces preciously depleted in the daughter ^{234}U by the recoil process. Reducing ground waters interact with uranium-rich grains of phosphorite, receiving the recoiling daughter ^{234}U. However, uranium is chemically insoluble in reducing waters; therefore, the uranium isotopic fingerprint of the water has a low concentration and a high activity ratio. After approximately 10^5 years, the phosphorite grains have developed a surficial rind that is deficient in daughter ^{234}U, as low as 50% (after several half-lives) right at the surface. If there is a subsequent change in water Eh from reducing to oxidizing, the rock surface becomes leached of its surficial rind and the karstic uranium isotopic fingerprint has a low activity ratio and a high concentration. This scenario is a possible explanation for what we find in the Woodville Karst Plain. This scenario also explains why trend lines can be found in karstic

areas. Deeper reducing waters with high activity ratios and low concentrations mix with oxidizing waters with low activity ratios and high concentrations to produce a mixing line that trends from lower left to the upper right of the activity ratio/reciprocal concentration plot. One can say that the reducing waters become oxidizing and result in the leaching because the concentration of uranium in the oxidizing waters dominates.

CONCLUSIONS

The study of uranium as a tracer in Wakulla Springs provides further understanding and documentation of the recharge areas and the circulation framework of the Floridan aquifer system in the Woodville Karst Plain. Generally, surface waters tend to have a high uranium activity ratio ($^{234}U/^{238}U$) and low uranium concentration while deep aquifer water has a low uranium activity ratio and high uranium concentration. The karstic waters of the Woodville Karst Plain, Florida, exhibit anomalously low $^{234}U/^{238}U$ ratios.

Wakulla Springs' pool water displays a mixture of leaching and non-leaching waters from the Woodville Karst Plain. Wakulla Springs pool samples have a low activity ratio and high concentration isotopic signature. Therefore, the main water source is the Floridan aquifer (tunnels A and C) because deep aquifer water has a low uranium activity ratio and high uranium concentration. Tunnels A and C seem to exert the most control upon the resultant isotopic spring signature. There is a dilute component in the Wakulla Springs' water. The diluting component has a moderate activity ratio and low concentration. This is recognized as rain or swamp water. Wakulla Springs represents a confluence of tunnel water and shallow horizon water.

Surface water and groundwater do interact from Tallahassee to the Woodville Karst Plain. The low uranium activity ratio found in the karstic deep ground water samples can also be evidence of oxidizing and reducing waters mixing and leaching away the long developed depletion rinds. The uranium fingerprint could be used to quantify surface and groundwater interaction. The uranium indexes of ground waters that vary over a season may have more surface water influence than samples without much variance. In the Woodville Karst Plain, evidence of surface water and groundwater interaction can also be found in the sinkholes, springs and their related cave systems. The pockets of tannic water found deep in the Wakulla Springs' tunnel A indicates that surface and groundwater are interacting, since most tannic water is formed at the surface in wet seasons. During wet seasons the uranium activity ratios are high. This may be due to the overwhelming capabilities of source tunnels to fingerprint the water during different atmospheric conditions.

Uranium results indicate that the pool water of Wakulla Springs can be readily interpreted as a simple mixture of the tunnels' waters and local ground and surface waters. Tunnel A and Tunnel C may be fed by groundwater underlying Woodville while Tunnel B and Tunnel D may be fed by the waters that underlie Tallahassee.

Wakulla Springs carry considerably more uranium (0.6 ppb) and are low in activity ratio (0.7-0.8). Waters discharged from Wakulla Springs are considered unusual in terms of its lower uranium activity ratios and higher uranium concentrations and the surficial waters from the surrounding area have a higher uranium activity ratio and lower uranium concentration.

ACKNOWLEDGEMENTS

We gratefully acknowledge the financial supports from the Florida Department of Environmental Protection (FDEP) and Department of Geology at the Florida State University. Thanks are due to Tom Miller, Adel Dabous, and Chris Werner for their assistance in collecting water samples. Jiun-Yee Yen is thanked for graphic production. The authors are indebted to Holly Williams for reviewing an earlier version of the manuscript and suggesting significant improvement. Riajul Islam provided a valuable critical review which led to significant improvements in the manuscript.

REFERENCES

Bonotto, D.M., and Andrews, J.N., 1993, The mechanism of $^{234}U/^{238}U$ activity ratio enhancement in karstic limestone groundwater: Chemical Geology, v. 103, p. 193-206.

Cherdyntsev, V.V., 1971, Uranium-234: Israel Program for Scientific Translations, Jerusalem, 234 p.

Clemens, L.A., 1988, Ambient groundwater quality in Northwest Florida, Part II: A case study in regional groundwater monitoring: Wakulla Springs, Wakulla County, Florida: Northwest Florida Water Management District, 25 p.

Cowart, J.B., and Osmond, J.K., 1977, Uranium isotopes in groundwater: their use in prospecting for sandstone-type uranium deposits: Journal of Geochemical Exploration, v. 8, p. 365-379.

Cowart, J.B., 1980, The relationship of uranium isotopes to oxidation/reduction in the Edwards carbonate aquifer of Texas: Earth and Planetary Science Letters, v. 48, p. 277-283.

Faure, G., 1986, Principles of Isotopes Geology (2nd ed.). New York: John Wiley & Sons, 589 p.

Hendry, C.W., and Sproul, C.R., 1966, Geology and groundwater resources of Leon County, Florida: Florida Geological Survey Bulletin, No. 47, 177 p.

Hussain, N., 1995, Supply rates of natural U-Th series radionuclides from aquifer solids into groundwater: Geophysical Research Letters, v. 22, p. 1521-1524.

Kaufman, M.I., Rydell, H.S., and Osmond, J.K. 1969, $^{234}U/^{238}U$ disequilibrium as an aid to hydrologic study of the Floridan aquifer: Journal of Hydrology, v. 9, p. 374-386.

Kigoshi, K., 1971, Alpha recoil Th-234: dissolution into water and the U-234/U-238 disequilibrium in nature: Science, v. 173, p. 47-48.

Kronfeld, J. Vogel, J.C., and Talma, A.S., 1994, A new explanation for extreme $^{234}U/^{238}U$ disequilibria in a dolomitic aquifer: Earth and Planetary Science Letters, v. 123, p. 81-93.

Kronfeld, J., and Vogel, J.C., 1991, Uranium isotopes in surface waters from southern Africa: Earth and Planetary Science Letters, v. 105, p. 191-195.

Lally, A.E., 1992, Chemical Procedures: In Uranium series disequilibrium: Applications to Environmental Problems (ed., M. Ivanovich and R. Harmon), 2nd Ed., p. 95-126, Clarendon Press, Oxford.

Lienert, C., Short, S.A., and von Gunten, H.R., 1994, Uranium infiltration from a river to shallow groundwater: Geochimica et Cosmochimica Acta, v. 58, p. 5455-5463.

Macesich, M.M., 1991, Uranium isotope disequilibrium study of Wakulla Springs: Unpublished masters thesis, Florida State University, Tallahassee, FL, 146 p.

Osmond, J.K., and Cowart, J.B., 1976, The theory and uses of uranium isotopes in hydrology: Atomic Energy Review, v. 14, p. 621-679.

Osmond, J.K., Rydell, H.S., and Kaufman, M.I., 1968, Uranium disequilibria in groundwater: an isotope dilution approach in hydrologic investigations: Science, v. 162, p. 997-999.

Rupert, F., and Spencer, S., 1988, Geology of Wakulla County, Florida: Florida Geological Survey Bulletin, No. 60, 46 p.

Stone, W., 1988, Wakulla Springs Conduit Map.

Whitecross, L.R., 1995, Groundwater and surface water interaction from Tallahassee, Florida to the Woodville Karst Plain: a study utilizing uranium disequilibrium modeling: Unpublished masters thesis, Florida State University, Tallahassee, FL, 98 pp.

Zielinski, R.A., Chafin, D.T., Banta, E.R., and Szabo, B.J., 1997, Use of ^{234}U and ^{238}U isotopes to evaluate contamination of near-surface groundwater with uranium-mill effluent; a case study in south-central Colorado, U.S.A.: Environmental Geology, v. 32, p.124-136.